NTNU – Trondheim
Norwegian University of
Science and Technology

Dynamic behavior of blow out preventer (BOP)

Zefeng Zhou

Geotechnics and Geohazards
Submission date: June 2012
Supervisor: Lars Olav Grande, BAT
Co-supervisor: Jan Holme, DNV

Norwegian University of Science and Technology
Department of Civil and Transport Engineering

NORWEGIAN UNIVERSITY OF SCIENCE AND TECHNOLOGY
DEPARTMENT OF CIVIL AND TRANSPORT ENGINEERING

Report Title: **Dynamic behavior of blow out preventer (soil and conductor system)**	Date: 19/12/2011 Number of pages (incl. appendices):			
	Master Thesis	✓	Project Work	
Name: Student Zhou Zefeng				
Professor in charge/supervisor: Lars Grandeaa				
Other external professional contacts/supervisors: Jan Holme (DNV)				

Abstract:
Nowadays, the offshore is very extensive and of great economic value for gross development. Typically all kinds of offshore structure will experience storm loading and need to consider the influence of cyclic loading. When cyclic loading is applied, the soil failure mechanism and strength of soil should be changed, which means the cyclic analysis need to perform in the way different from static analysis. If designer ignore the effect of cyclic load, the failure or large plastic deformation will occur with increasing the number of cyclic loading.

I have studied the lateral displacement of conductor under influence of cyclic loading, and the numble of cyclic loading is 10, 100, 1000 and 10000 in the calculation, respectively. Moreover the soil modulus will be calculated from Matlab with the elastic pile theory (Lars Grande, Phd thesis 1976). During the cyclic loading, the soil degradation should be considered, therefore, the modified P-y curve for influence of cyclic loading is included which describes the change of soil. In terms of calculation, there are two types of BOP, 450 tons and 250 tons, meanwhile the horizontal cyclic loading equal to 2000 kN which is performed on BOP.

Then the natural frequency analysis is performed in last chapter. The natural frequencies of the conductor, BOP, wellhead and soil system have a significant influence on the system stability. The frequencies that correspond to the maxima magnification factor M which means the vibration could be magnified. Without the damping impact, when a frequency of cyclic loads equal to the natural frequencies of the system, the magnification factor will be infinite, while the damping is included, the factor will also

meet a peak value when the two kinds of frequencies meet each other. Consequently the analysis will be operated for both two types BOP in this calculation. And The multiple-degree-of freedom model is operated in this case, therefore, the conductor is considered as an elastic pile which is divided into several elements and that conductor only connect soil with springs is included in this chapter.

Further work in connection to soil plasticity theory, can be developing more accuracy deflection calculation. When cyclic loading is considered, the plastic zone is developing around conductor, therefore the new soil model need to use for practical project.

Keywords:

1. Cyclic loading
2. Soil degradation
3. nonlinear soil behavior
4. Modified P-y curve

_____

(signature)

MASTER DEGREE THESIS

Spring 2012

for

Student: <<Zhou Zefeng>>

<< Dynamic behaviour of blow out preventer (soil and conductor system)>>

BACKGROUND

Nowadays, the offshore is very extensive and of great economic value for gross development. Typically all kinds of offshore structure will experience storm loading and need to consider the influence of cyclic loading. When cyclic loading is applied, the soil failure mechanism and strength of soil should be changed, which means the cyclic analysis need to perform in the way different from static analysis. If designer ignore the effect of cyclic load, the failure or large plastic deformation will occur with increasing the number of cyclic loading.

TASK DESCRIPTION

I have studied the lateral displacement of conductor under influence of cyclic loading, and the numble of cyclic loading is 10, 100, 1000 and 10000 in the calculation, respectively. Moreover the soil modulus will be calculated from Matlab with the elastic pile theory (Lars Grande, Phd thesis 1976), and the deflection will be calculated on Matlab and SPLICE and Geosuite. Moreover the natural frequency analysis will also be done in this paper.

General about content, work and presentation

The text for the master thesis is meant as a framework for the work of the candidate. Adjustments might be done as the work progresses. Tentative changes must be done in cooperation and agreement with the professor in charge at the Department.

In the evaluation thoroughness in the work will be emphasized, as will be documentation of independence in assessments and conclusions. Furthermore the presentation (report) should be well organized and edited; providing clear, precise and orderly descriptions without being unnecessary voluminous.

The report shall include:

- Standard report front page (from DAIM, http://daim.idi.ntnu.no/)
- Title page with abstract and keywords.(template on: http://www.ntnu.no/bat/skjemabank)
- Preface

- Summary and acknowledgement. The summary shall include the objectives of the work, explain how the work has been conducted, present the main results achieved and give the main conclusions of the work.
- Table of content including list of figures, tables, enclosures and appendices.
- If useful and applicable a list explaining important terms and abbreviations should be included.
- The main text.
- Clear and complete references to material used, both in text and figures/tables. This also applies for personal and/or oral communication and information.
- Text of the Thesis (these pages) signed by professor in charge as Attachment 1..
- The report musts have a complete page numbering.

Advice and guidelines for writing of the report is given in: "Writing Reports" by Øivind Arntsen. Additional information on report writing is found in "Råd og retningslinjer for rapportskriving ved prosjekt og masteroppgave ved Institutt for bygg, anlegg og transport" (In Norwegian). Both are posted posted on http://www.ntnu.no/bat/skjemabank

Submission procedure

Procedures relating to the submission of the thesis are described in DAIM (http://daim.idi.ntnu.no/). Printing of the thesis is ordered through DAIM directly to Skipnes Printing delivering the printed paper to the department office 2-4 days later. The department will pay for 3 copies, of which the institute retains two copies. Additional copies must be paid for by the candidate / external partner.

On submission of the thesis the candidate shall submit a CD with the paper in digital form in pdf and Word version, the underlying material (such as data collection) in digital form (eg. Excel). Students must submit the submission form (from DAIM) where both the Ark-Bibl in SBI and Public Services (Building Safety) of SB II has signed the form. The submission form including the appropriate signatures must be signed by the department office before the form is delivered Faculty Office.

Documentation collected during the work, with support from the Department, shall be handed in to the Department together with the report.

According to the current laws and regulations at NTNU, the report is the property of NTNU. The report and associated results can only be used following approval from NTNU (and external cooperation partner if applicable). The Department has the right to make use of the results from the work as if conducted by a Department employee, as long as other arrangements are not agreed upon beforehand.

Tentative agreement on external supervision, work outside NTNU, economic support etc.
Separate description to be developed, if and when applicable. See http://www.ntnu.no/bat/skjemabank for agreement forms.

Health, environment and safety (HSE) http://www.ntnu.edu/hse
NTNU emphasizes the safety for the individual employee and student. The individual safety shall be in the forefront and no one shall take unnecessary chances in carrying out the work. In particular, if the student is to participate in field work, visits, field courses, excursions etc. during the Master Thesis work, he/she shall make himself/herself familiar with " Fieldwork HSE Guidelines". The document is found on the NTNU HMS-pages at http://www.ntnu.no/hms/retningslinjer/HMSR07E.pdf

The students do not have a full insurance coverage as a student at NTNU. If you as a student want the same insurance coverage as the employees at the university, you must take out individual travel and personal injury insurance.

Start and submission deadlines
The work on the Master Thesis starts on January 16, 2012

The thesis report as described above shall be submitted digitally in DAIM at the latest at 3pm June 11, 2012

Professor in charge: name

Other supervisors: name

Trondheim, January 16, 2012.

_____

Professor in charge (sign)

PREFACE

This Master Thesis was performed at the Geotechnical division at NTNU the spring semester and it studies that dynamic behavior of blow out preventer (soil and conductor system). The topic is proposed by DNV Foundation group by Jan Holme who wanted a study of cyclic loading affecting on conductor.

The Master Thesis is a further work of the master project (Lateral deformation of clay and sand due to cyclic loading in connection with structural well integrity during well operations) which had been done in 2011-2012 winter semester and proposed by DNV Foundation group. The topic in master project mainly studied the lateral deflection of conductor without scour in sand condition, and the calculation is performed on Geosuite and SPLICE programs.

During the Master Thesis work I have been helped by many, with inputs, suggestions and valuable discussions. I especially want to thank my supervisors Lars Grande (NTNU) and Jan Holme (DNV) who have encouraged me and been helpful with testing and suggestions. I will thank Prof. Thomas Benz and Siamak.Feizikhankandi(DNV) who help me resolve the many difficult topics in the paper.

ABSTRACT

Nowadays, the offshore is very extensive and of great economic value for gross development. Typically all kinds of offshore structure will experience storm loading and need to consider the influence of cyclic loading. When cyclic loading is applied, the soil failure mechanism and strength of soil should be changed, which means the cyclic analysis need to perform in the way different from static analysis. If designer ignore the effect of cyclic load, the failure or large plastic deformation will occur with increasing the number of cyclic loading.

I have studied the lateral displacement of conductor under influence of cyclic loading, and the numble of cyclic loading is 10, 100, 1000 and 10000 in the calculation, respectively. Moreover the soil modulus will be calculated from Matlab with the elastic pile theory (Lars Grande, Phd thesis 1976). During the cyclic loading, the soil degradation should be considered; therefore the modified P-y curve for influence of cyclic loading is included which describes the change of soil. In terms of calculation, there are two types of BOP, 450 tons and 250 tons, meanwhile the horizontal cyclic loading equal to 2000 kN which is performed on BOP.

Then the natural frequency analysis is performed in last chapter. The natural frequencies of the conductor, BOP, wellhead and soil system have a significant influence on the system stability. The frequencies that correspond to the maxima magnification factor M which means the vibration could be magnified. Without the damping impact, when a frequency of cyclic loads equal to the natural frequencies of the system, the magnification factor will be infinite, while the damping is included, the factor will also meet a peak value when the two kinds of frequencies meet each other. Consequently the analysis will be operated for both two types BOP in this calculation. And The multiple-degree-of freedom model is operated in this case, therefore, the conductor is considered as an elastic pile which is divided into several elements, and that conductor only connect soil with springs is included in this chapter.

Further work in connection to soil plasticity theory, can be developing more accuracy deflection calculation. When cyclic loading is considered, the plastic zone is developing around conductor, therefore the new soil model need to use for practical project.

Contents

LIST OF FIGURES

LIST OF TABLES

1 INTRODUCTION

Cyclic loading is very important for offshore foundation design, which has a significant influence on the shear strength of soil. Typically all kinds of offshore structure will experience storm loading and need to consider the influence of cyclic loading. When cyclic loading is applied, the soil failure mechanism and strength of soil should be changed, which means the cyclic analysis need to perform in the way different from static analysis. If designer ignore the effect of cyclic load, the failure or large plastic deformation will occur with increasing the number of cyclic loading. This master thesis will discuss that the lateral deflection of BOP (blow out preventer) wellhead under cyclic loading, natural frequency analysis of the conductor and soil system, and soil degradation problems.

Figure 1-1 The BOP, wellhead and soil-conductor system

In this paper, the calculation is operated in SPLICE, Geosuite, and Matlab programs and some Matlab codes for analysis will be shown in Appendix.

1.1 PROBLEM IN THIS THESIS

Large lateral wellhead movements have been observed on Deepsea Atlantic. The well system was made at Troll in December of 2009 and January of 2010. The riser system, BOP and conductor were equipped with measuring devices including accelerometers, strain gauges and motion sensors. Figure 1-1,

Figure 1-3 and Figure 1-4show drilling operations performed at Troll at three different time segments. In Figure 1-2 It is clearly that no deformation or degradation of the wellhead support is found at the seabed, while 9 hours later in operation the degradation of wellhead support had been taking place, with the numble of cyclic loading increasing the plastic deformation is increasing as well, which is shown in Figure 1-3. The degradation is a trumpet shaped hole around the conductor. Figure 1-4 shows that the trumpet shape hole has increased in size and plastic deformation continue to increase, which can be observed in the ROV video that the wellhead and conductor system less restrained to move, as a consequence of the diminished support level.

In the meantime, with the various frequencies dynamic loading, the several-degree of freedom system will have the different model shape and deflection at seabed. Moreover if the frequency of loading is close to natural frequency of system, the resonance might occur which is the worst condition for structure. In addition the paper will also give a suggestion about the change of natural frequency with the increase of numble of cyclic loading for the multiple DOFs system, and the gap between soil and conductor is also mentioned in this dynamic analysis.

Figure 1-2: Troll well 31/2-12 U Drilling with BOP

Figure 1-3: Troll well 31/2-12 U Drilling with BOP

Figure 1-4: Troll well 31/2-12 U Drilling with BOP

This paper will use the case with sand soil to calculate the lateral deformation when the conductor applied the cyclic loading. The calculation model is based

on several assumptions. The conductor is assumed to have linear elastic response which means the conductor fatigue problem and cement cracking in tension or compression are not included. It is assumed that cyclic lateral loads are applied at the flex-joint (BOP) and it is the two-way cyclic lateral load. The Long and Vanneste described the behavior of the pile for four phases. During the first quarter-cycle, the magnitude of lateral load varies from a value of zero to a maximum horizontal load.

It is assumed that the resistance to pile deflection is provided by the soil along the loading side of the pile while the soil along the opposite side of the pile maintains contact by flowing with the pile. When the load decreases to zero during the second quarter-cycle, the soil pressure along the opposite direction decreases to an active state. The cohesionless soil was also assumed to flow and prevent a gap, to ensure contact with pile surface, by contrast, the soil with scour and without scour will both be considered in this analysis, therefore the sediment transport theory should be included in this paper (chapter 3). Similar assumptions to maintain the contact between soil and pile surface were also made in the third and fourth quarter-cycles. To maintain the contact at all times is also assumed in this study, at same time the influence of gap is also included in the calculation in chapter 6. This assumption may not reflect actual conductor and soil conditions due to a cyclic loading, especially for a two-way loading. However, the simplifications are needed to keep the model tractable.

2 SOIL DEGRADATION

When cyclic loading is applied on structure or pile foundation, the soil around the foundation will experience soil degradation and deformation of soil will increase as well. The bearing capacity of a soil will probably decrease with the cyclic loading occurring, and significantly the lateral deflection under cyclic loading increase with number of cyclic and become larger than the deflection under static loading at the same load when the cyclic horizontal loading is considered, which is reason why the cyclic loading tends to break down the soil structure and cause a volumetric reduction in the soil.

2.1 SOME SOIL MODELS FOR CYCLIC LOADING

In the simple model (equivalent linear model), the soil subjected to symmetric cyclic loading could indicate a hysteresis loop of the type, and the inclination of the loop depends on the stiffness of the soil, meanwhile, the average value over the entire loop can be approximated by the secant shear modulus G_{sec}. The characteristic parameters G_{sec} will vary with cyclic shear strain amplitude. However, in the equivalent linear model , the soil is treated as a linear viscoelastic materials(model shown in Figure 2-1) which means the linear

springs exist between soil and pile and stiffness rising with depth increase, so the shear strain is proportional to the shear stress.

Viscous (fluid-like) and elastic (solid like) characteristics

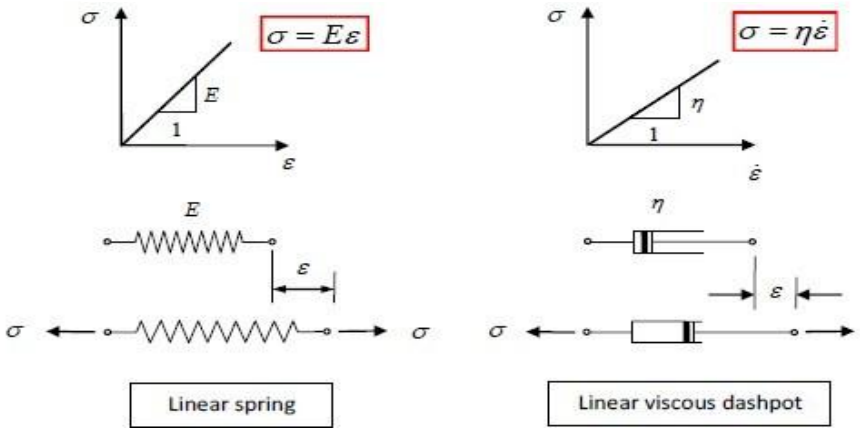

Figure 2-1 A linear viscoelastic materials model

From previous laboratory tests, the cyclic strain amplitude, void ratio, mean principal effective stress, plasticity index, overconsolidation ratio, and numble of loading cycles have an influence on soil stiffness. Actually in real soil, the soil has nonlinear behavior which means variable stiffness exist for different load steps (Figure 2-2).

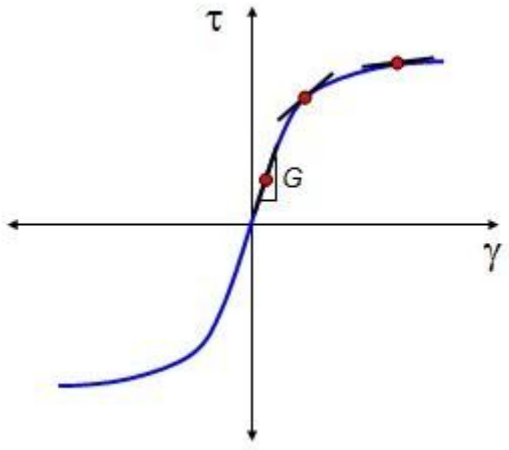

Figure 2-2 Nonlinear, elastic behavior

The stiffness of the soil is usually characterized by the maximum shear modulus G_{max}, which is mobilized at low strains, and a modulus reduction curve and shows how the shear modulus decreases at larger strains (Figure 2-3).

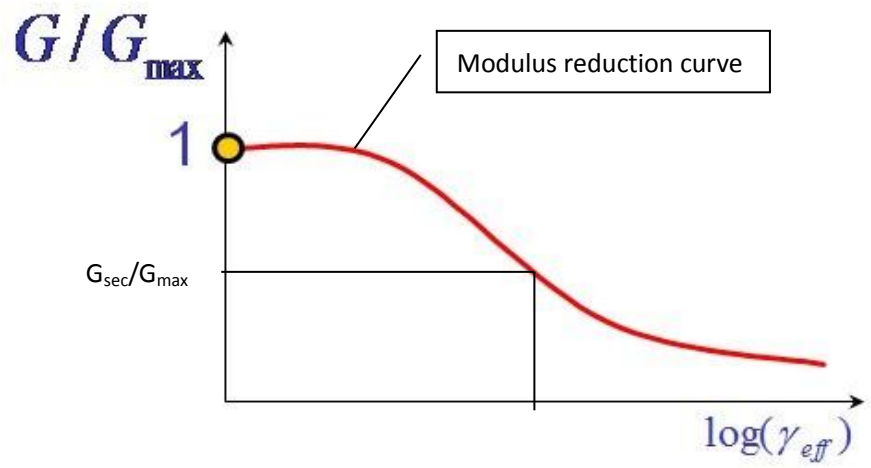

Figure 2-3 The shear modulus reduction

With more and more requirement in accuracy of soil behavior, more advanced models could help us to be better to simulate the behaviors than simple models. The simple models are always too dominated by theory of elasticity, while soil mostly follows the plastic property. When operating advanced models there are more material properties to handle, and determining these properties could be more difficult than for the simple models.

In advanced soil models, the soil behavior under cyclic loading will be indicated accurately, and the advanced soil models could include the elastic and plastic deformation with yield surface, hardening rule and flow rule established. The yield surface indicates that the soil reaches a limitation at which irreversible or plastic deformations start to appear. The hardening rule demonstrate the change of shape of yield surface after plastic deformation occurring, and flow rule relates increments of plastic strain to increments of stress and defines the plastic strain rate tensor in a way that ensures non-negative dissipation. Consequently this model is more general than others and could more useful to describe the soil behavior, cyclic and static loading, high or low strain rates, and linear or cyclic nonlinear models.

2.2 THE BEHAVIOUR OF CLAY UNDER CYCLIC LOADING

In clay condition, the soil is always considered as undrained, the volumetric changes will be prevented by the low volumetric compressibility of water, and it also refers to the effective stress theory($\sigma = \sigma' + \mu_w$), so the normal stresses that were carried by the soil will then be transferred to the pore water and the effective stresses. When the period of cyclic loading is enough small, the pore water will be carried the majority of stresses and effective stresses in the soil will decrease accordingly. As shown in below Figure 2-4, it is clear that the

permanent water pressure increases with number of the constant amplitude cyclic shear stress (average stress $\tau_a = 0$) increasing. The growth of the shear strain amplitude during cyclic loading reflects a gradual deterioration of the clay with an excess pore pressure associated, which may also have an influence on break-down of electrochemical bonds between soil particles under the cyclic loading.

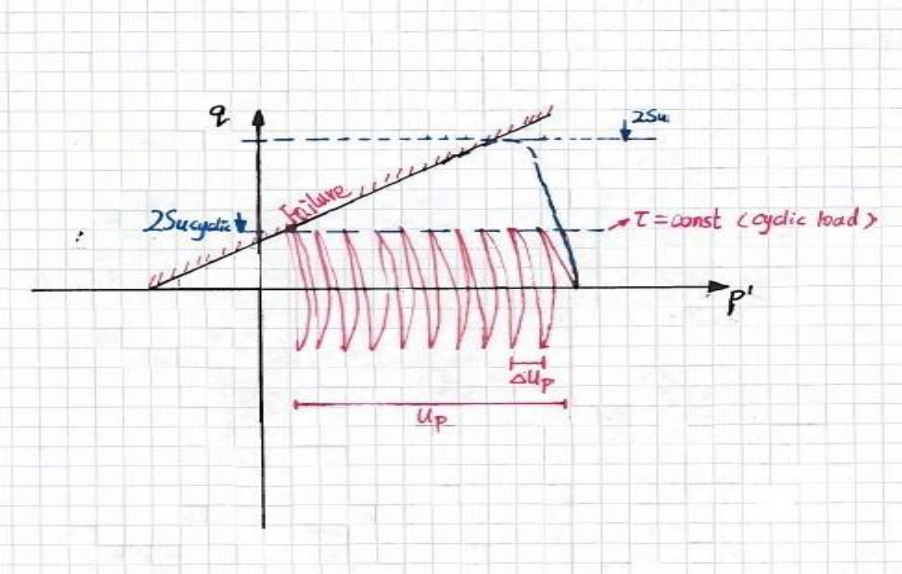

Figure 2-4 Soil undrained strength under the cyclic loading

2.2.1 CYCLIC SHEAR STRENGTH AND FAILURE

From the previous lab tests, the cyclic shear strength and failure mechanism under cyclic loading depend mainly on the combination of average and cyclic shear stresses. When average stress $\tau_a = 0$, the cyclic stress will mainly influence on the soil stability with combination of unloading and reloading conditions. While the average stress isn't zero, below certain critical value, the average stress would enhance the stability of soil when cyclic is same as before. Consequently the cyclic strength of an element of soil depends on the relationship between the τ_{ave} and τ_{cyc}.

τ_{ave} is low, so unidirectional strains will accumulate slowly, and the average strains will also be low (Figure 2-5).

- When τ_{ave} is high, substantial unidirectional strains can develop even when the cyclic shear stress is small.
- When τ_{ave} is zero, no unidirectional strain will develop, so failure must be defined in terms of the cyclic shear strain.
- When τ_{ave} >0, both r_{cyc} and r_{ave} will depend on τ_{ave} and τ_{cyc}, respectively, in which r_{cyc} depends predominantly on τ_{cyc} and the number of cycles, and r_{ave} depends predominantly on τ_{ave} and the number of cycles.
- When τ_{cyc} is large, the amplitude of the cyclic strain become large.

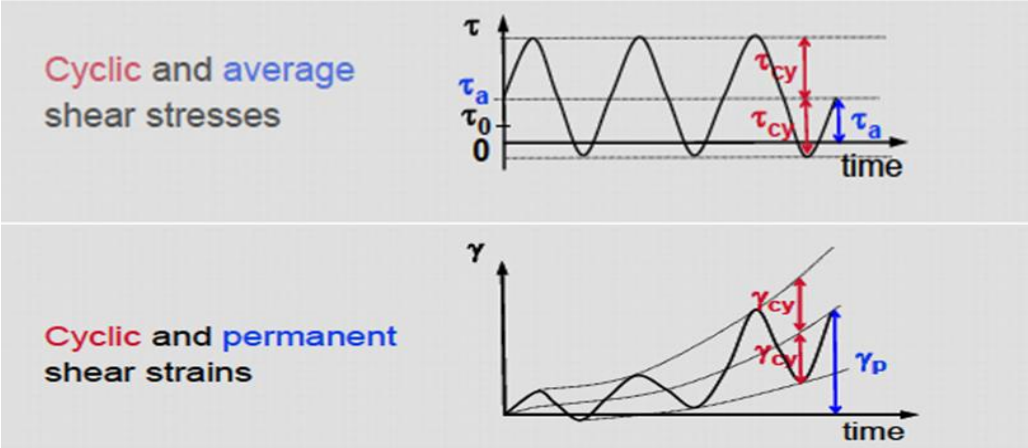

Figure 2-5 Cyclic stress and permanent shear strains

Meanwhile, the definition of failure could be defined in different ways. In static condition, when large deformation of soil exceed the critical limit value, soil is define failure (Ultimate Limit State and Serviceability limit states), while the cyclic loading is applied on the foundation, the r_{cyc} and r_{ave} will produce τ_{ave} and τ_{cyc}, respectively, as a result, clearly the strength of soil under cyclic loading should be defined including the limited critical values of r_{cyc} and r_{ave} or combination of the two. So the failure of soil during cyclic loading will consider the influence of r_{cyc} and r_{ave} with different number of cyclic loading.

3 SEDIMENT TRANSPORT

3.1 INTRODUCTION

When the cyclic loadings applied(waves and wind), the structure of sediment which is around the conductor or offshore foundation piles is always broken down and cause a volumetric reduction in the soil, and the particles will flow away.

The movement of sediment particles is defined as sediment transport, and the problem will cause decrease of the capacity of surface soil, and the gap between pile and soil comes more and more with the cyclic applied continuously. The movement of sediment particles depends on the characteristics of the transported materials (grain-size and fall velocity) and cyclic loading, which theory will be shown below. There it is shown that sediment particles will start moving when a so-called critical velocity (or critical shear stress) is exceeded. The bed shear stress in the seabed soil is the result of the combined wave-current motion and pile motion caused by wind loading. In general, there are two transport modes included: bed load and suspended load.

- **Bed load transport**: the transport of sediment particles in a thin layer close to the bed. The particles are in more or less continuous contact with the bed. Bed load transport at low shear stresses the movement of particles are entire contacted with soil layer, while at higher shear stresses, a whole layer of sediment is moving on a plane bed which is always called sheet flow.

- **Suspended load transport**: the transport of particles suspended in the water without any contact with the bed, and the particles are supported by turbulent diffusive forces.

3.2 SEDIMENT PROPERTIES

In this topic, obviously, there are two conditions of sediment transport shown. Firstly the water in the gap between soil and conductor (or piles) will be pumped by the movement of conductor (or piles), therefore the water have an influence on the movement of soil particles. Secondly the wave-current motion also increases velocity of the sediment particles. In this two condition, actually the forces on the soil particle need to analysis.

In terms of the grain size, it is also an important property of sediment. Two important parameters for soil are the D_{50}, and the ratio between two particle diameters (D_1/D_2), where the D_x is defined as the sediment particle diameter for which x% by weight is finer.

With an assumption that the water condition is still and clear, the sediment particle will be put in the water with various accelerations and velocity, for a while, the acceleration of particle will decrease and reach zero, at this time the velocity keep constant which is called fall velocity. This velocity can be obtained from the balance between the downward directed gravity force F_G and the upward directed drag force F_D as indicated in Figure 3-1 below.

In case of a perfect condition, the force F_G which need to minus the buoyancy and the upward directed force are equal to the drag force defined by F_D. This equilibrium is obtained by the balance of forces when the acceleration is zero.

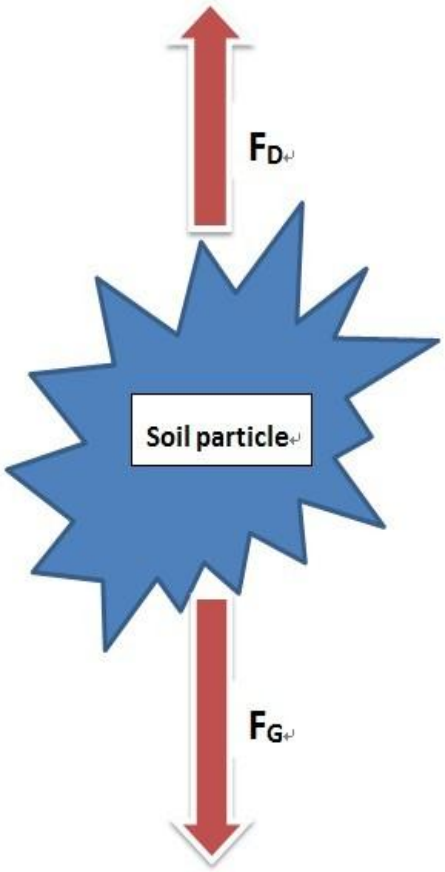

Figure 3-1 Forces on a particle in clear water

$$F_G = (\rho_s - \rho) * g * (\frac{\pi}{6} * D^3)$$ .....Equation 3-1

Where:

ρ_s: Mass density of the particle [kg/m*3]

ρ: Mass density of the surrounding fluid [kg/m*3]

D: Particle diameter [m]

$$F_D = \frac{1}{2} * C_D * \rho * \omega_S^2 * (\frac{\pi}{4} * D^2)$$ .....Equation 3-2

Where:

C_D: The drag coefficient

ω_s: The particle fall velocity [m/s]

And also the fall velocity ω_s is given by:

$$\omega_s = \sqrt{\frac{4*(s-1)*g*D}{3*C_D}}$$ .....Equation 3-3

As the Equation 3-3 shown, the drag coefficient, particle size and density have the key influence on the value of fall velocity, ω_s. Meanwhile the drag coefficient mainly depends on the grain Reynolds number (Equation 3-4) and the drag coefficient is as a function of Reynolds number (Figure 3-2):

$$R_e = \frac{\omega_s * D}{v} \quad \text{.....Equation 3-4}$$

Where:
v: kinematic viscosity coefficient

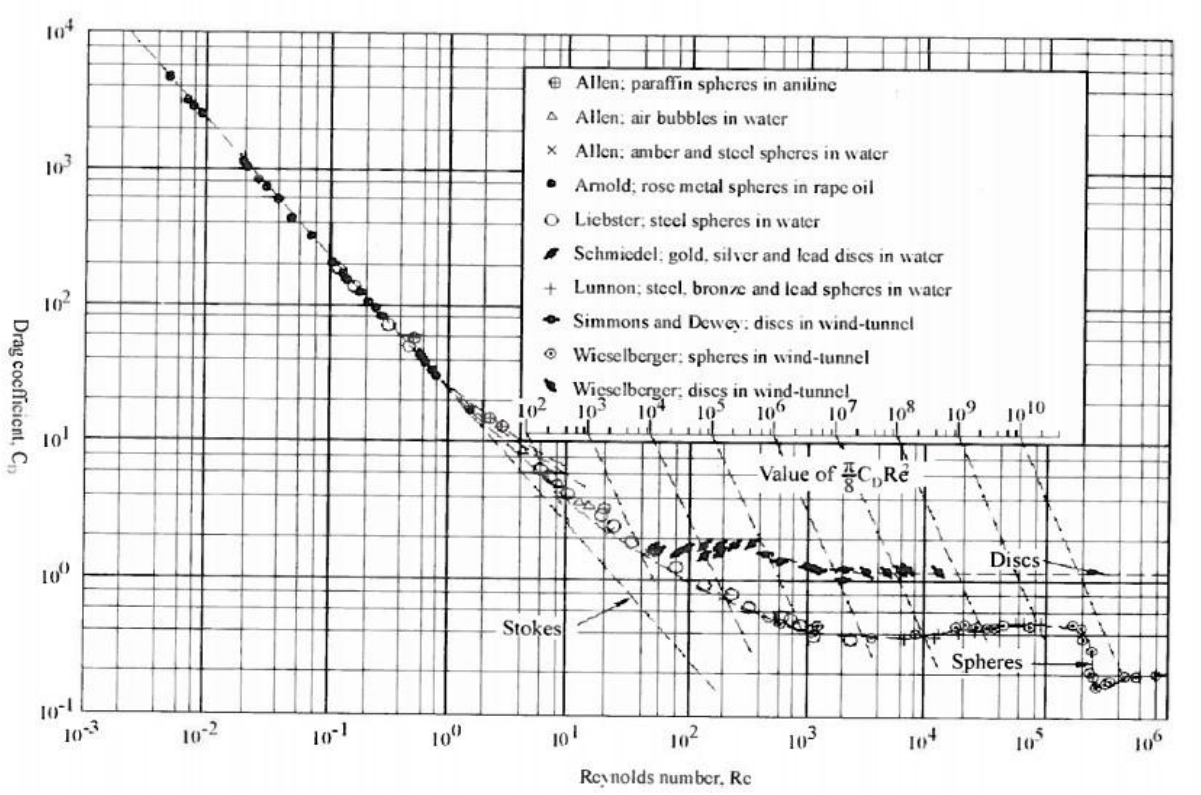

Figure 3-2 Drag coefficient as a function of Reynolds number

From the Figure 3-2, with the low grain Reynolds number (Re<0.1 to 0.5) which is named Stokes-range, the fall velocity depends on the square of the grain diameter, the relative density and the kinematic viscosity coefficient, by contrast, with high Reynolds number (400<Re<2*e5) which is named Newton range, the fall velocity depends on the square root of the grain diameter and the relative density without influence of kinematic viscosity coefficient.

3.3 INITIATION MOTION

From the basic theory given by Paintal, in reality, the condition is very complicate, and actually there is not a characteristic value at which the motion and suspension suddenly begins, however in terms of statistic the value fluctuated around an average value.

When the sediment can be transported, the critical value of motion is met. Moreover the water movement makes a large enough shear stress which describes the point of initiation of motion. Therefore, if the condition is greater than the critical value, grains move and roll with the water movement. In addition, a single grain is acted with various forces which can be divided into the drag force, lift force and the gravity force, see Figure 3-3.

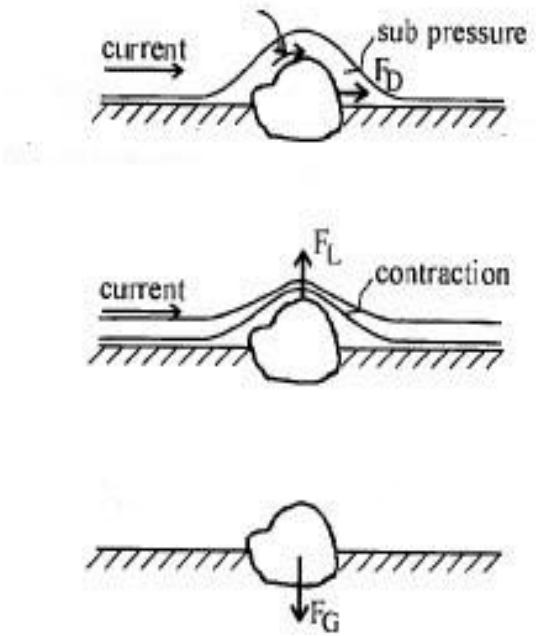

Figure 3-3 forces on a single grain in a stable situation: drag force, lift force and the gravity force

3.3.1 SHIELDS CURVE

In order to determine the critical shear stress in the grain, the critical shields parameter θ_{cr} can be deduced (Equation 3-5):

$$\theta_{cr} = \frac{\tau_{b,cr}}{(\rho_s - \rho) * g * D} = C \quad \text{.....Equation 3-5}$$

Where:

$\tau_{b,cr}$: The critical bottom shear stress.
ρ_s: Mass density of the particle.
ρ: Mass density of the surrounding fluid.
D: Particle diameter.

The constant C has to be obtained by experiment. Shields test performed on a flat bed, and he defined the critical bed shear stress as the bed shear stress at which the measured transport rates equal to zero. Meanwhile Shields found the constant C is approximate 0.05 which was a weak function of the grain

Reynolds number defined as:

$$\mathrm{Re} = \frac{u_* * D}{v} \quad \text{..... Equation 3-6}$$

Where:

u_*: Shear stress velocity

D: Diameter

v: Kinematic viscosity coefficient

From the Equation 3-6 above, the Shields curve could be show as Figure 3-4:

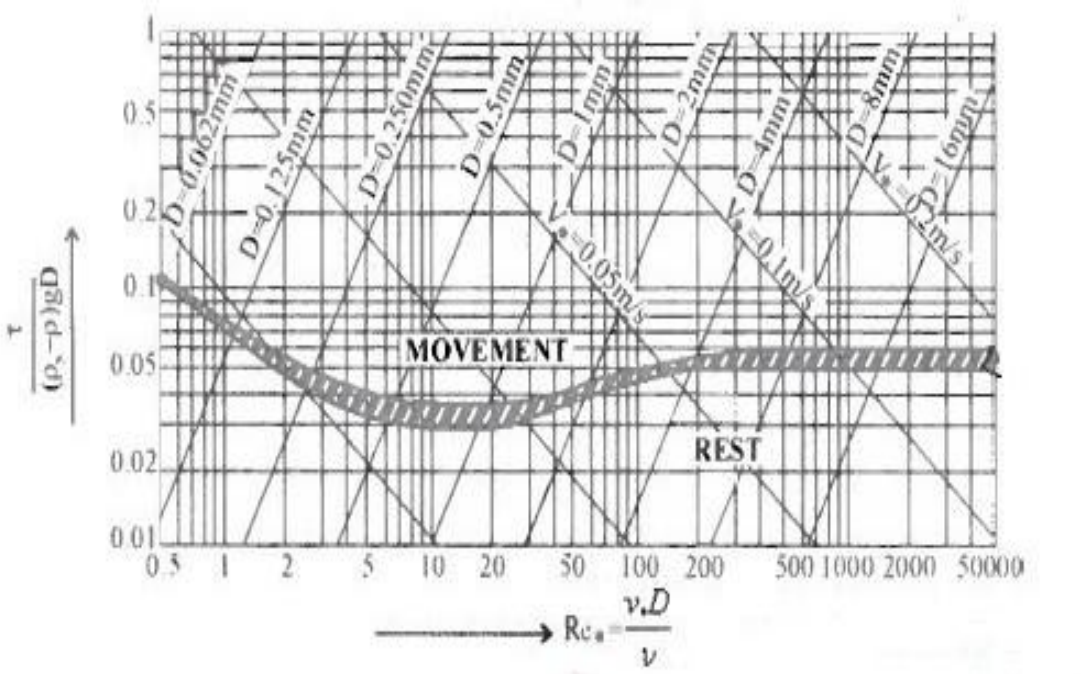

Figure 3-4 Shields curve for initiation of motion

The Shields curve indicates the relation between the critical mobility Shields' parameter and the dimensionless particle Reynolds number. Hydraulic condition is given by the Reynolds number which is depended on the grain size and the shear velocity, obviously the initiation of motion will occur when mobility Shields' parameter is greater than the critical value.

3.3.2 HJULSTRöM CURVE

Hjulström had published the Hjulström diagram at 1935 and modified at 1939 which shows the threshold flow velocity as a function of the particle diameter for a 100 cm water level flow. Average speed is practically a good parameter to be determined. It is not a unique parameter, as the velocity distribution in a channel will be dependent on cross-sectional shape, varying roughness, water depth, etc. Hjulström chart is the best known in this regard, see Figure 3-5. It is from 1935 and is based on experiments with relatively sand and relatively constant water depth. Values from the diagram are called critical speed.

Curve provides a useful overview of how particle size and speed will determine: persistent erosion, relatively constant sediment transport and deposition of mass. The narrow area of the figure shows a transition state with incipient erosion or detachment of particles when the speed is increasing. When the grain size reaches the area, increasing the speed is limited because of the cohesive forces. If the rate instead decreases beyond this range, the particles already in motion could continue to move down to the bottom line in the chart.

The Hjulström diagram could be approximated with the 2 empirical equations for threshold flow velocity and the deposition velocity as derived by Miedema (2010).

$$U_c = 1.5 * \left(\frac{v}{D}\right)^{0.8} + 0.85 * \left(\frac{v}{D}\right)^{0.35} + 9.5 * \frac{R_d * g * D}{(1 + 2.25 * R_d * g * D)}$$

$$U_d = 77 * \frac{D}{(1 + 24 * D)}$$

Where:
R_d: The relative submerged specific density
D: Sphere, particle or grain diameter

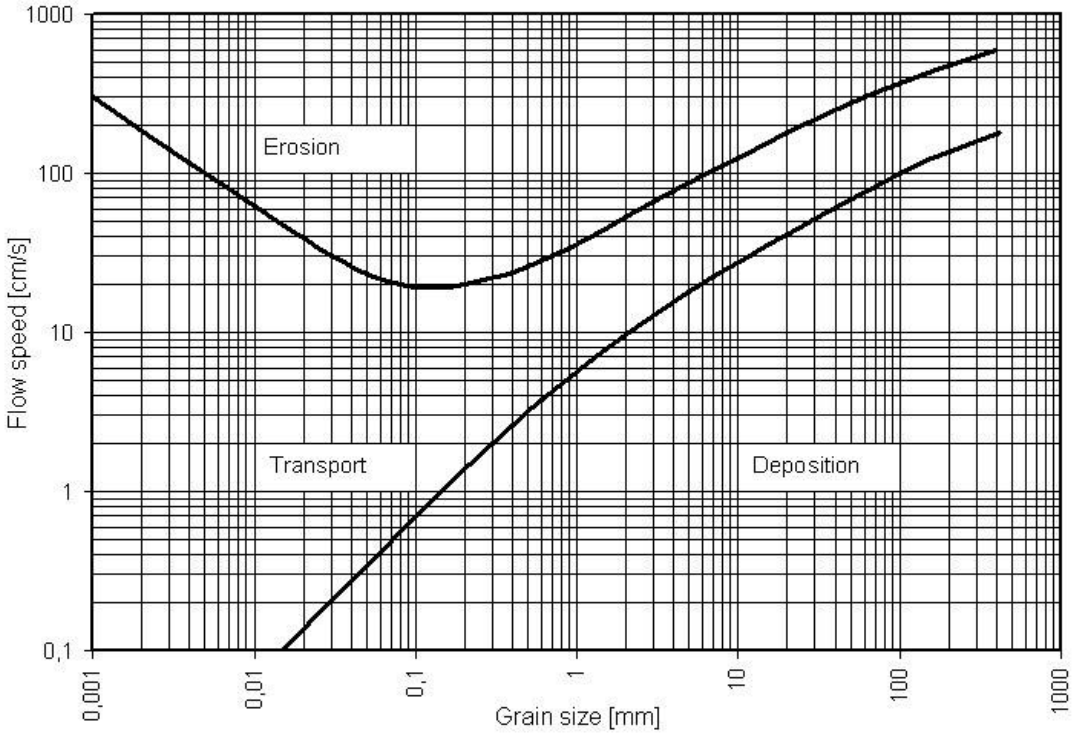

Figure 3-5 Hjulström curve for the boundary between erosion and deposition

4 MODIFIED NONLINEAR STATIC P-Y CURVE FOR CYCLIC LOADING

The lateral resistance loads are important for the offshore foundation (conductor), whether static or cyclic. Wind, waves, storms, earthquakes, and water pressures, may produce cyclic lateral loads to pile supported offshore foundation, while the wind turbine monopile foundation is designed to subject static lateral loads.

4.1 MODIFIED NONLINEAR STATIC P-Y CURVE FOR SAND (API CODE)

From API code, the static P-y curve and lateral bearing capacity for sand could be demonstrated as below:

4.1.1 THE ULTIMATE LATERAL BEARING CAPACITY FOR SAND

The ultimate lateral bearing capacity for sand has been found to vary from a value at shallow depths determined by Equation 4-1 to a value at deep depths determined by Equation 4-2. At a given depth the equation giving the smallest value of p_u should be used as the ultimate bearing capacity.

$$p_{us} = (C_1 X + C_2 D)\gamma' X \quad \text{..... Equation 4-1}$$

$$p_{ud} = C_3 D\gamma' X \quad \text{..... Equation 4-2}$$

Where

p_{us}: Ultimate resistance (force/unit length) (s=shallow, d=deep)

γ': Effective soil weight, in weight density units

X: Depth

$\emptyset'$: Angle of internal friction in sand

$C_1 C_2 C_3$: Coefficients determined from Figure3-1

D : Average pile diameter from surface to depth

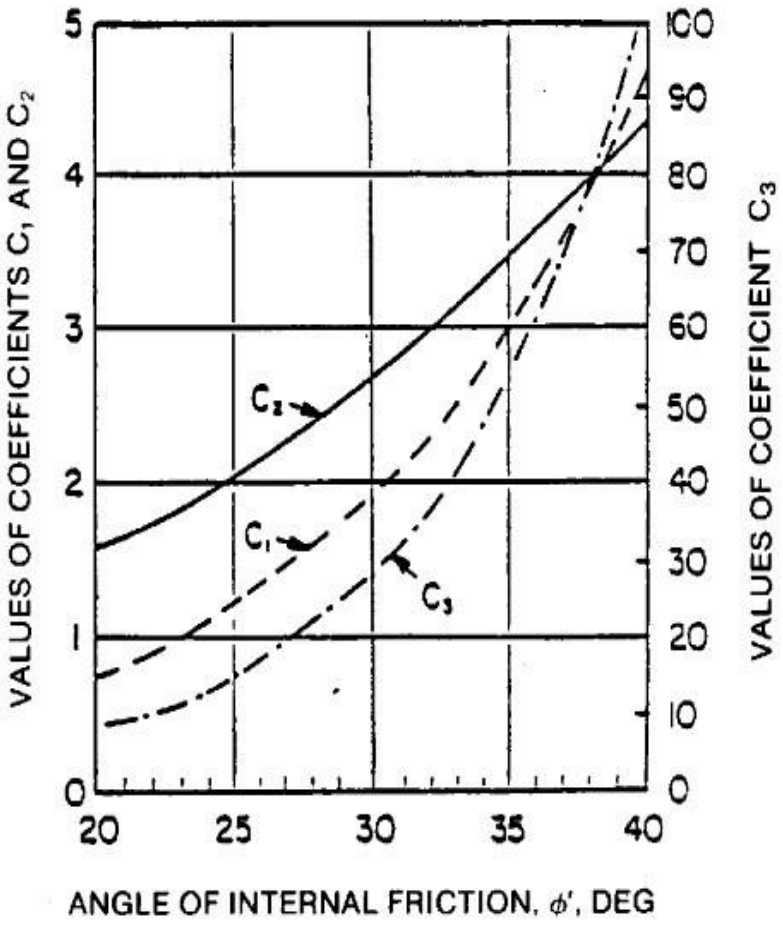

Figure 4-1 COEFFICIENTS AS FUNCTION OF ϕ'

4.1.2 THE LOAD-DEFLECTION (P-Y) CURVE FOR SAND

The lateral soil resistance-deflection (P-y) relationship for sand is also nonlinear and in the absence of more definitive information may be approximated at any specific depth X, by the following expression:

$$P = Ap_u \tanh\left[\frac{k*X}{A*p_u}y\right]. \quad \text{.....Equation 4-3}$$

Where:

A : Factor to account for cyclic or static loading continued. Evaluated by:

A = 0.9 for cyclic loading.

A = $(3.0 - 0.8\frac{X}{D})$ $\geq$0.9 for static loading.

p_u: Ultimate bearing capacity at depth X in units of force per unit length

k : Initial modulus of subgrade reaction in force per volume units. Determine from Figure 4-2 as function of angle of internal frictionϕ',

y: Lateral deflection

X: Depth

Table 4-1: Reaction coefficient, k (kN/m3)

Soil type	Over ground water table	Under ground water table
Silty clay	1000-3000	500-2000
Loose sand	5000	4500
Middle fast sand	22000	15000
Dense sand	60000	34000

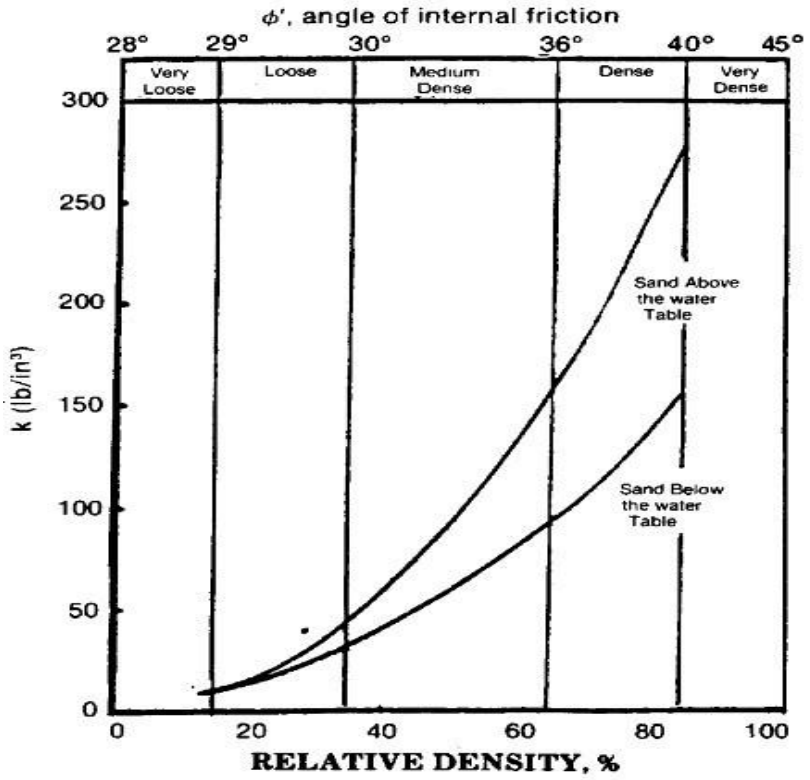

Figure 4-2 The k value with angle of internal friction

4.1.3 MODIFIED NONLINEAR STATIC P-Y CURVE FOR SAND

The static P-y cures were proposed by Reese et al.(1974), based on some full-scale cyclic pile load test results. And then the more detailed and accurate research on the effect of cyclic lateral loads on piles in sand was performed by Long and Vanneste using degradation of the static P-y curve (DSPY). The method based on the results of 34 full-scale tests. After that, the Lin & Liao apply a strain superposition procedure for predicting the pile-permanent horizontal displacement which contains effect of number of lateral load cycles on strain ratio and effect of depth coefficient on degradation parameter, t.

$$P_N = P_1 * N^{(\alpha-1)t}$$

$$y_N = y_1 * N^{(\alpha t)}$$

$$t_1 = 0.17 * F_L * F_I * F_D$$

$$t_2 = 0.032 * \left(\frac{L}{T}\right) * F_L * F_I * F_D$$

(With effect of depth coefficient on degradation parameter)

Where:
P_N: The soil resistance for N cycle of load
(α): Controls the relative contribution of soil resistance and deflection to decrease the soil reaction modulus.
(t_1): Degradation parameter
(t_2): Degradation parameter (with effect of depth coefficient on degradation parameter)
L: The pile length
T: The pile/soil relative stiffness ratio

4.2 MODIFIED NONLINEAR STATIC P-Y CURVE FOR CLAY (API CODE)

From API code, the static P-y curve and lateral bearing capacity for soft clay could be demonstrated as below:

4.2.1 LATERAL BEARING CAPACITY FOR SOFT CLAY

In the API code, for static lateral loads the ultimate unit lateral bearing capacity of soft clay P_u has been found to vary between $8*S_u$ and $12*S_u$ except at shallow depths where failure occurs in a different mode due to minimum overburden pressure. Cyclic loads cause deterioration of lateral bearing capacity. In the absence of more definitive criteria, the following is recommended:

P_u increase from $3*S_u$ to $9*S_u$ as X increase from 0 to XR according to:

$$Pu = 3 * Su + \gamma X + J * \frac{Su * X}{D}$$

$$Pu = 9 * Su \text{ for } X \geq X_R$$

Where:

Pu: Ultimate resistance, in stress units

S_u: Undrained shear strength of undisturbed clay soil samples, in stress units

D: Pile diameter

Γ: Effective unit weight of soil, in weight density units

J : Dimensionless empirical constant with values ranging from 0.25 to 0.5 having been deter units mined by field testing. A value of 0.5 is appropriate for Gulf of Mexico clays.

X_R: Depth below soil surface to bottom of reduced resistance zone (a condition of constant strength with depth).

4.2.2 THE LOAD-DEFLECTION (P-Y) CURVES FOR SOFT CLAY

Lateral soil resistance- deflection relationships for piles in soft clay are generally nonlinear. The P-y curves for the short-term static load case may be generated from the following table:

Table 4-2 P-y curve for soft clay

P/Pu	Y/Yc
0	0
0.5	1
0.72	3
1	8
1	∞

Where:

P¨ Actual lateral resistance, in stress units

y: Actual lateral deflection

y_c : 2.5 E,D

For the case where equilibrium has been reached under cyclic loading, the P-y curves may be generated from following:

X>XR	
P/Pu	Y/Yc
0	0
0.5	1
0.72	3
0.72	∞

X<XR	
P/Pu	Y/Yc
0	0
0.5	1
0.72	3
0.72X/XR	15
0.73X/XR	∞

4.3 MODIFIED STATIC P-Y CURVE FOR CYCLIC LOADING WITH THEORY EQUATIONS

When static P-y curve have been gotten, the next step is to modify it including the cyclic loading influence. Here, the Equations (4-4 and 4-5) which are operated for cyclic loading P-y curve is given by (Long & Vanneste 1994) which are based on 34 soil tests. And also it needs to include the influence of degradation parameter t including effects of cyclic loading ratio, installation and soil density (Table 4-4 to Table 4-6).

$$P_N = P_1 * N^{(\alpha-1)t} \quad \text{.....Equation 4-4}$$

$$y_N = y_1 * N^{(\alpha t)} \quad \text{.....Equation 4-5}$$

4.3.1 DAGRADATION PARAMETER t

The degradation parameter, t, is an empirical parameter which depends on the soil tests and as blow:

$$t_1 = 0.17 * F_L * F_I * F_D \quad \text{.....Equation 4-6 (Long \& Vanneste 1994)}$$

$$t_2 = 0.032 * \left(\frac{L}{T}\right) * F_L * F_I * F_D \quad \text{.....Equation 4-7 (Lin \& Liao 1999)}$$

Here, the parameter t_2 is modified based on depth coefficient $\frac{L}{T}$ (Table 4-3).

Table 4-3 Parameter t versus L/T (Lin & Liao 1999)

Case (1)	Method of installation (2)	t versus L/T	Number of pile tests
(a)	Driven (RH)=0, loose	t=0.042L/T	5
(b)	Driven (RH)=0, dense	t=0.032L/T	1
(c)	Driven (RH)=0, medium	t=0.045L/T	6
(d)	Backfilled (RH)=0, loose	t=0.076L/T	2
(e)	Sonic vibrated (RH)=0, loose	t=0.035L/T	1
(f)	Vibrated (RH)=0, loose	t=0.010L/T	2
(g)	Driven (RH)=0, dense	t=0.011L/T	1
(h)	Driven (RH)=0, dense	t=0.004L/T	1
(i)	Backfilled and compacted (RH)=-1, medium	t=0.003L/T	1

Table 4-4 Effect of cyclic load ratio on parameter FL (Long & Vanneste 1994)

Load ratio R_H	F_L
-0.1(two-way loading)	0.2
-0.25	0.4
0.0	1.0
0.5	1.0
1.0	0.0

Where:

$$R_H=H_{min}/H_{max}$$

- R_H=0, a pile cycled from 0 to one way loading is calculated to have a cyclic load ratio 0.
- R_H=-1, equal load magnitude in both directions has a ratio -1.
- R_H=1, a pile loaded statically would have a value of 1.

Table 4-5 effect of installation on parameter FI (Long & Vanneste 1994)

Method of installation	F_I
Driven	1.0
Vibrated	0.9
Backfilled	1.4
Backfilled and compacted	1.0
Drilled	1.3
Precycled (regardless of installation)	1.0

Table 4-6 Effect of soil density on parameter FI (Long & Vanneste 1994)

Soil density	F_D
Loose(contractive)	1.1
Medium	1.0
Dense	0.8
Precycled (regardless of density)	1.0

In this case, the degradation parameter t is (Table 4-8) :

Table 4-7 The t value estimated

t value	F_L	F_I	F_D
0.0374	0.2	1	1.1

The degradation parameter t is estimated based on soil tests and comparing the value from the equation above. From the 34 tests done by Long and Vannests, fifty percent of the measured values of t exceeded values of t predicted using. When estimated value of t is multiplied by 1.4, just 16%of the

measured values exceed those predicted. If it need that a mere 3% of the measured t values exceed the predicted value, it needs to select 2 to multiply the value.

4.3.2 CORRECT FACTOR a

In the nonlinear P-y curve, with the depth increasing, the P-y curve is various. When the cyclic loading is applied, the values of P and y are changed at the same time to describe the soil degradation. Here, the value of a controls the relative contribution of soil resistance and deflection to decrease the soil reaction modulus. The range of "**a**" is from 0 (P value changed only) to 1 (y value changed only).

In the calculation, clearly the values of "**a**" are 0.9, 0.6 and 0.1in equations to express the influence of a on soil reaction (Table 4-8).

Table 4-8 Correct factor for a=0.1, 0.6 and 0.9

a	P	y
0.1	P_N=P_1*N^(-0.7t)	y_N=y_1*N^((0.3t))
0.6	P_N=P_1*N^(-0.4t)	y_N=y_1*N^((0.3t))
0.9	P_N=P_1*N^(-0.1t)	y_N=y_1*N^((0.3t))

5 ANALYSIS AND CALCULATION ON GEOSUITE AND SPLICE

5.1 ASSUMPTIONS IN CYCLIC CALCULATION

In this case, actually there are many factors should be considered. However it mainly finds the result of the cyclic loading and soil degradation, consequently there are assumption for simplifying the case.

- The conductor fatigue problem and cement cracking in tension or compression are not included.
- The cyclic lateral loads are applied at the weight center of BOP and it is the two-way cyclic lateral load with same amplitude.
- The soil is assumed to flow and prevent a gap, to ensure contact with pile surface.
- The period of load is 10s, so this problem is cyclic analysis.

5.2 CASE TO BE MODELLED

The problem is modeled by Geosuite 2011 and is sketched in Figure 5-1. In the real case the structure consists of a conductor with an inner casing and cement (grout) between the casing and conductor and outside the conductor, while in this project the model simplify the conductor as a steel tubes and an equivalent pile with an equivalent length L_{eq}=50m which is assumed to have a Young's modulus E_s=210 G_{pa}, outer diameter D=0.9144m and thickness t=0.439 m (Figure 5-2).

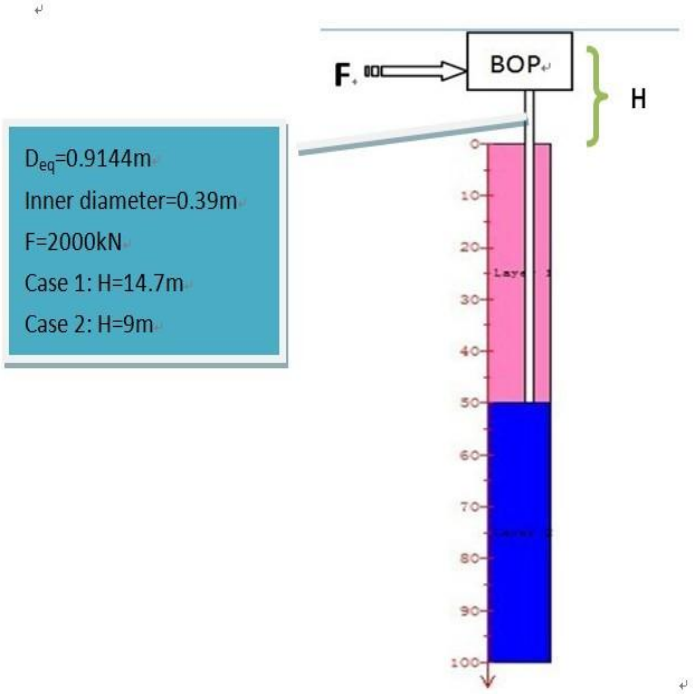

Figure 5-1 Model in Geosuite 2011

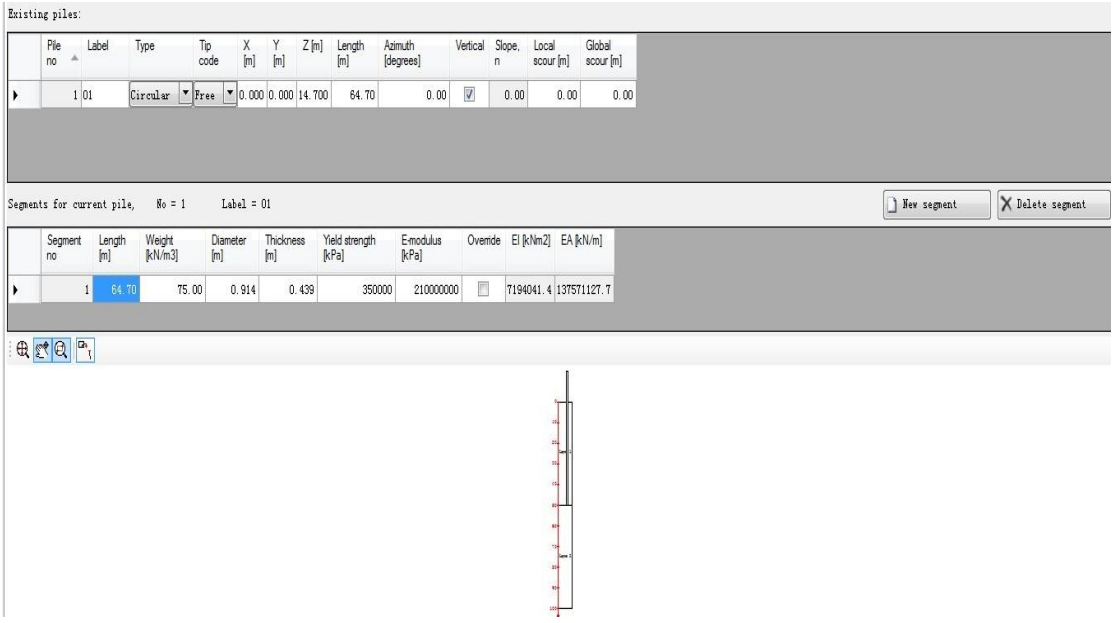

Figure 5-2 Conductor model in Geosuite

The BOP is assumed to be exposed to an equivalent horizontal load QH=2000 kN at the flex joint, that is located 14.7 m above mud-line, while as usually the height of BOP is arranged from 6 m (250 ton) to 13 m (450 ton), in the meanwhile the wellhead is located 3m above mud-line. Consequently there are two models with different BOP height.

5.3 SOIL CONDITIONS

At the case site, the water depth is about 325m, and the soil consists of soft clay, sandy clay, sand and many gravels and stones with low plasticity. In this project it assumed the soil condition is mainly sand (Figure 5-3 and Table 5-1).

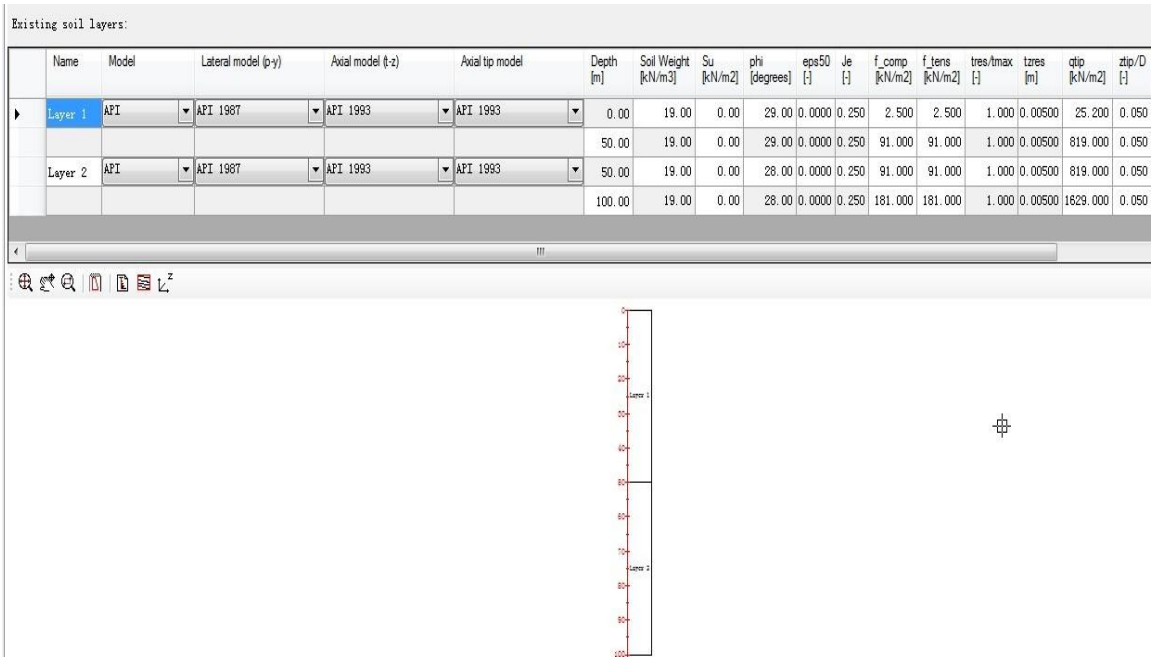

Figure 5-3 Soil profile and parameters in Geosuite

Table 5-1 Soil parameters

Soil depth	Friction angle (degree)	API-J parameter	Side friction in compression(Kpa)	Side friction in tension(Kpa)	Residual side friction	Tip bearing stress	Ztip/D
0	29	0.25	2.5	2.5	0.005	25	0.05
50	29	0.25	91	91	0.005	819	0.05
50	28	0.25	91	91	0.005	819	0.05
100	28	0.25	181	181	0.005	1629	0.05

5.4 GEOSUITE 2011 PILE PROGRAM FOR STATIC LOADING CALCULATION

Before it considers that the cyclic loading influence on soil behavior, the static loading is applied on the conductor, and no soil degradation is included (Figure 5-4).

Table 5-2 Cases for BOP

Case 1 with BOP 13m	H=14.7 m
Case 2 with BOP 6m	H=9 m

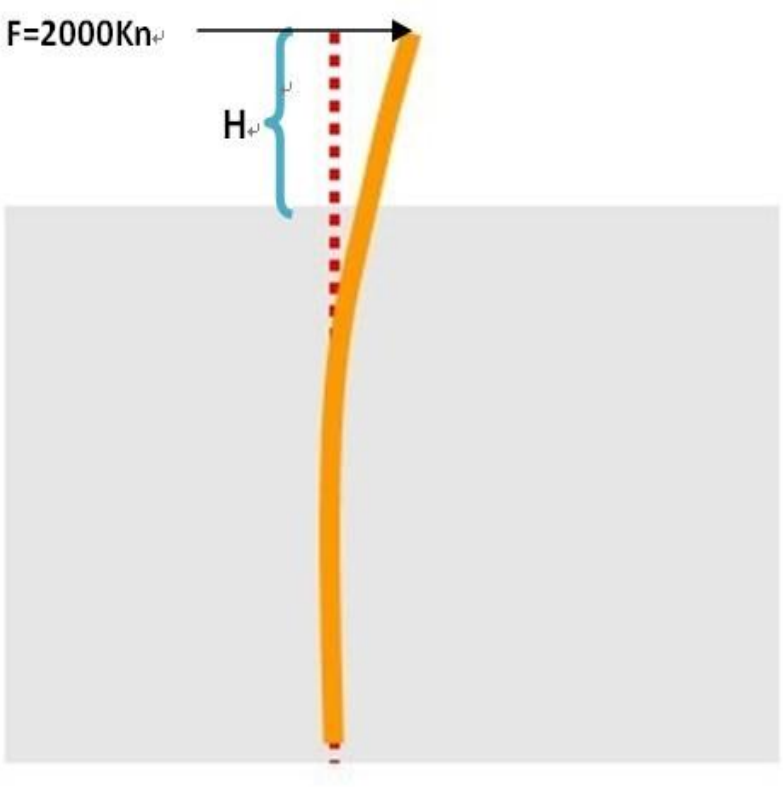

Figure 5-4 Static loading model

5.5 SUMMARY AND RESULTS

The surrounding soil of the conductor has been checked to have strength to resist the presented static and cyclic loads, and mainly the lateral deflection of the conductor has been checked in the same time. The static analysis and cyclic analysis have been operated.

The case has been analyzed considering the following methods:

- With and without including cyclic loading effect.
- Including the correct factor an effect for a= 0.1, 0.6 and 0.9, respectively.

5.5.1 STATIC ANALYSIS IN GEOSUITE

In static loading (2000 kN) applied on the BOP, the deflection of conductor at mud-line is approximate 45cm, while the maximum deflection of the tube is 1.82m at 14.7m above the mud-line.

In Geosuite, the soil is layered into 110 layers from 0m to 100m below the mud-line. For simplification, the depth bottoms of layers (0.91m, 1.82m, 2.73m, 5.45m and 10.9m) are selected for modifying nonlinear P-y curve (Figure 5-6).

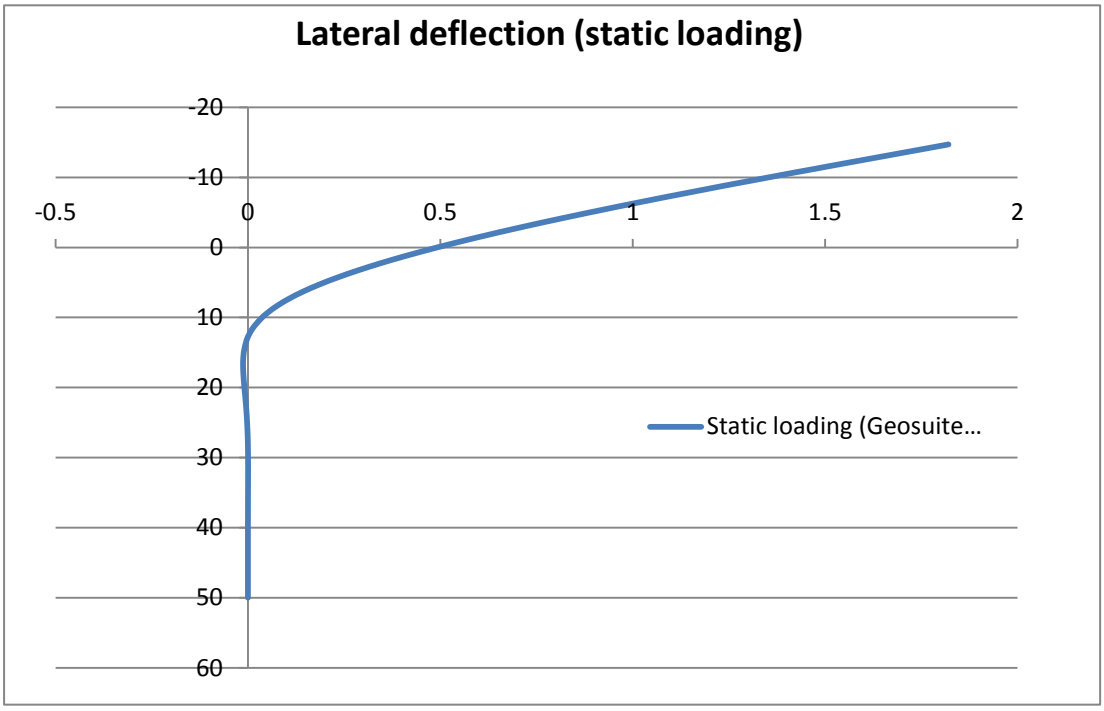

Figure 5-5 Lateral deflection (static loading)

The static P-y curve is produced by API 1987 code, which indicates the soil capacity is rising with the depth increasing. And also it seems that the nonlinear springs are modeled at the different soil depth to simulate the nonlinear behavior of real soil. The peak P stresses are indicated for different depth in Table 5-3 below.

Table 5-3 The peak P stresses

Depth (m)	Peak P stress (kpa)
0.91	12.55
1.82	56.85
2.73	126.8
5.45	342.9
10.9	1204
25.4	3742
50.9	7858

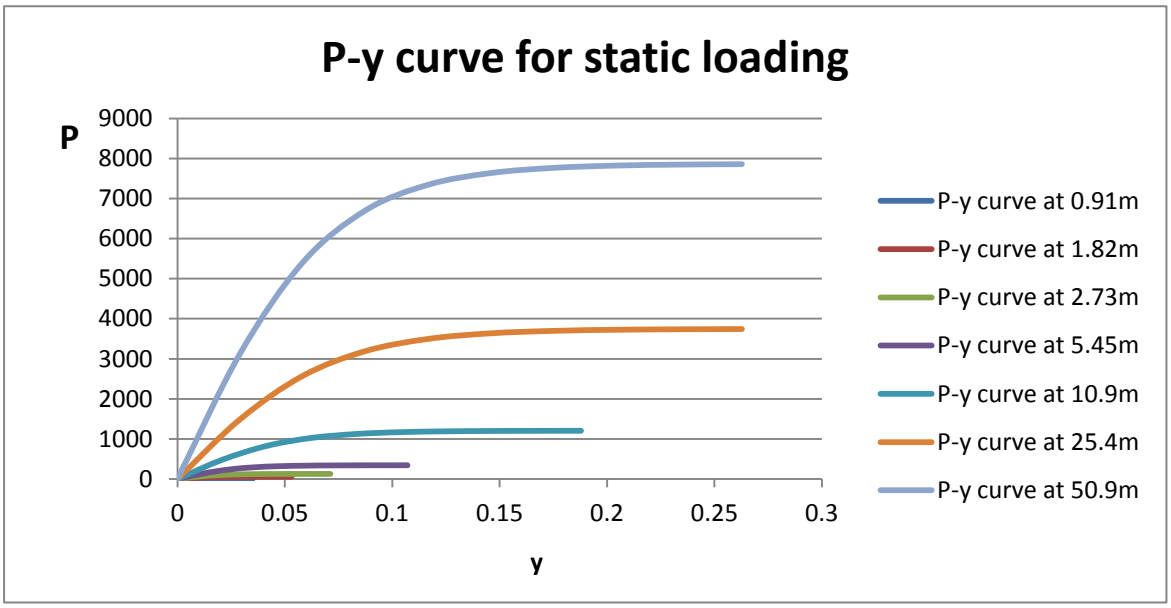

Figure 5-6 P-y curve for static loading

5.5.2 CYCLIC LOADING ANALYSIS IN SPLICE

The cyclic loading analysis operating, we input the manual P-y curve data into the SPLICE program to obtain the lateral deflection of conductor for 10, 100, 1000 and 10000 cyclic loading respectively. In the meantime the effects of degradation parameter t and correct factor a are included in this analysis.

5.5.2.1 CYCLIC ANALYSIS FOR t=0.0374 (a=0.6)

The analysis performs the $t= 0.17 * F_L * F_I * F_D$=0.0374, and uses the constant a=0.6 which is the recommended value after comparing the LISM (Linearly Increasing Soil Modulus) method (Long & Vanneste 1994). The later deflections in different numble of cycle are indicated below (Figure 5-7). The huge deflection is caused by the soft material of tube and the theoretically wrong result which means that there is little effect of cyclic loading for t=0.0374 is for introducing the effect of cyclic loading only. Then the other calculation will use the steel tube.

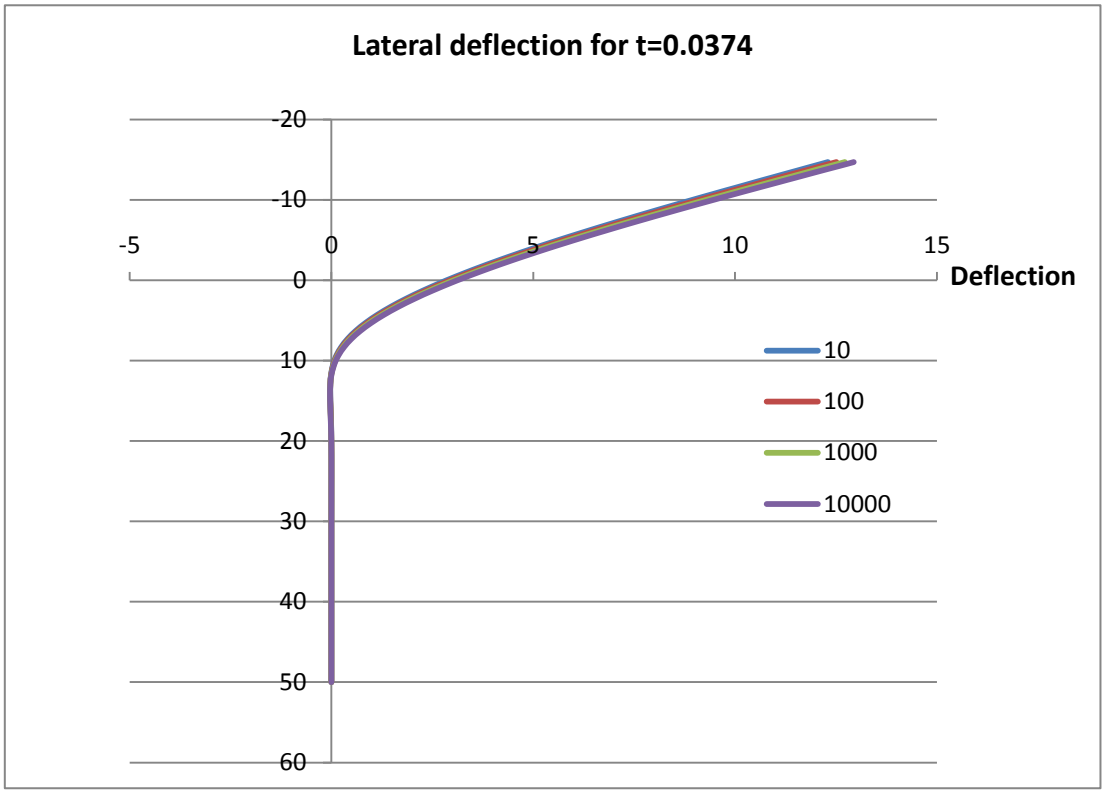

Figure 5-7 Cyclic loading lateral deflection for t=0.0374

5.5.2.2 CYCLIC ANALYSIS FOR t=0.0748 (a=0.6)

When estimated value of t is multiplied by 1.4, just 16%of the measured values exceed those predicted. If it need that a mere 3% of the measured t values exceed the predicted value, it needs the value multiply by 2, which will amplifying the deflection (Figure 5-9 and Figure 5-10). And also the modified P-y curve is showed below (Figure 5-8).

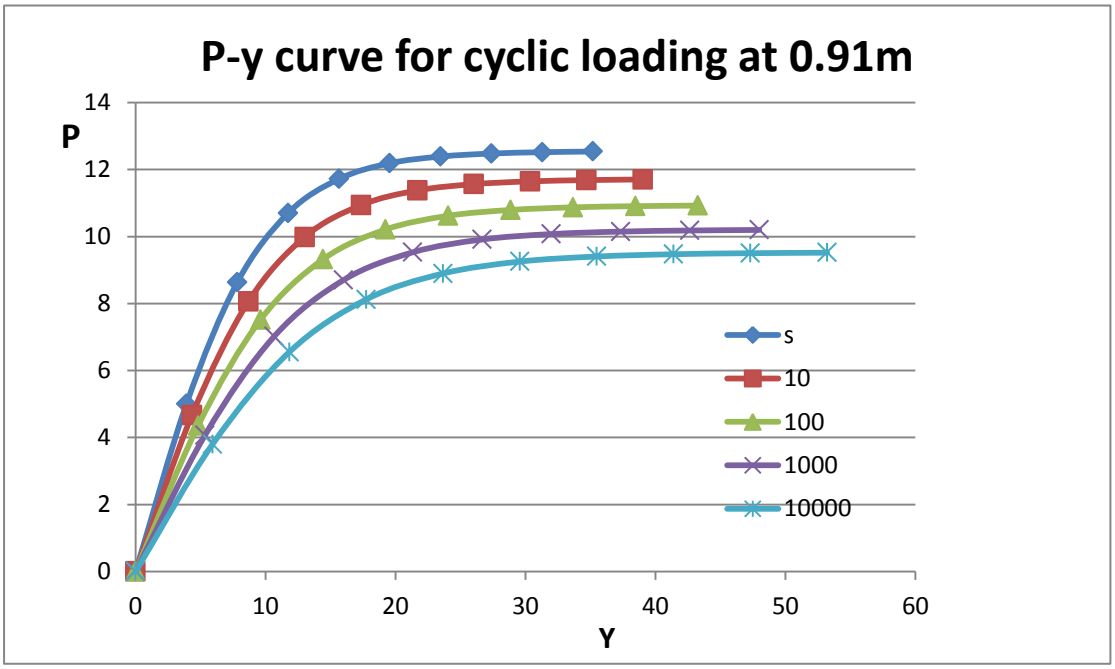

Figure 5-8 Modified P-y curve for cyclic loading at 0.91m

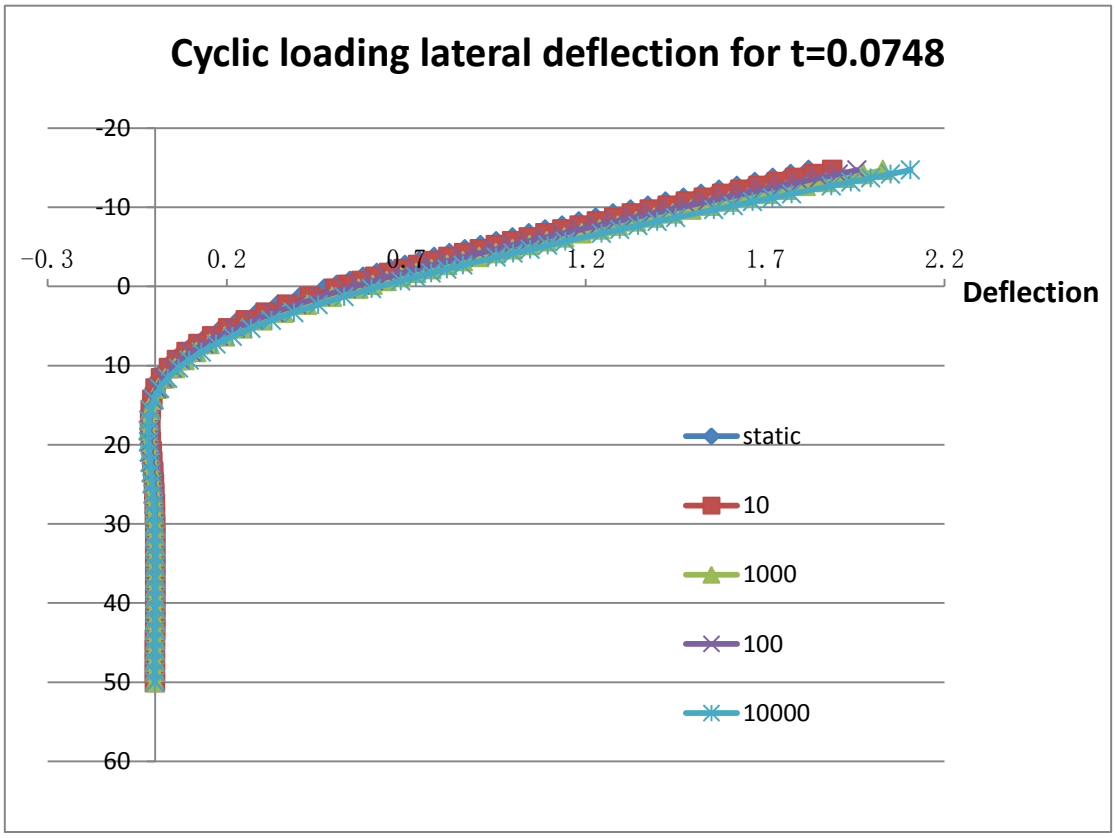

Figure 5-9 Cyclic loading lateral deflection for t=0.0748

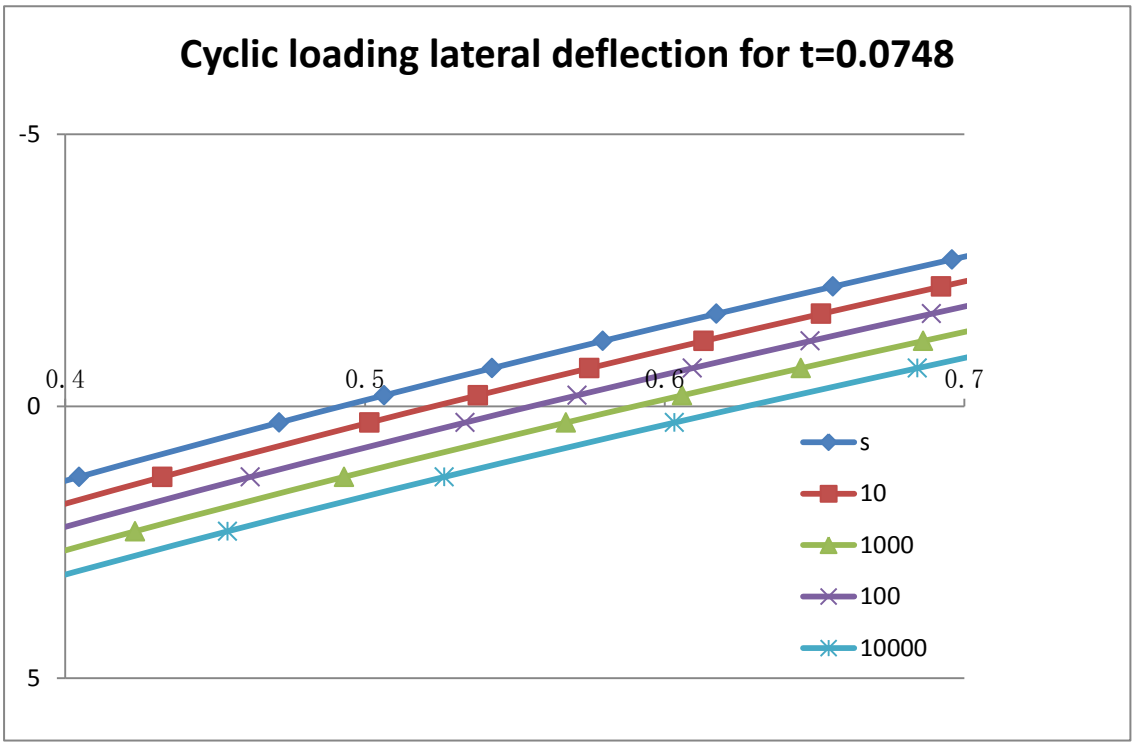

Figure 5-10 Cyclic loading lateral deflection for t=0.0748

Comparing the deflection of conductor in static, cyclic loading=10 increase

6.7%, cyclic loading=100 increase 13.49%, cyclic loading=1000 increase 20.66% and cyclic loading=10000 increase 28.3%, respectively.

Table 5-4 Lateral deflection at mud-line

Cyclic loading	Lateral deflection at mud-line(cm)
static	47
10	50.15
100	53.34
1000	56.71
10000	60.3

5.5.2.3 CYCLIC ANALYSIS FOR t=0.0748 (a=0.1 and a=0.9)

When the correct factor a=0.1 is applied into the Equation (4-6 and 4-7), it means that the value mainly control P value under cyclic loading. By contrast, the correct factor a=0.9 mainly control y value and there is little effect on P value. The result of a=0.1 and a=0.9 are indicated below Figure 5-11 and Figure 5-14, respectively.

$$P_N = P_1 * N^{(-0.9)t} \quad \text{..... (a=0.1)}$$

$$y_N = y_1 * N^{(0.1t)} \quad \text{..... (a=0.1)}$$

$$P_N = P_1 * N^{(-0.1)t} \quad \text{..... (a=0.9)}$$

$$y_N = y_1 * N^{(0.9t)} \quad \text{..... (a=0.9)}$$

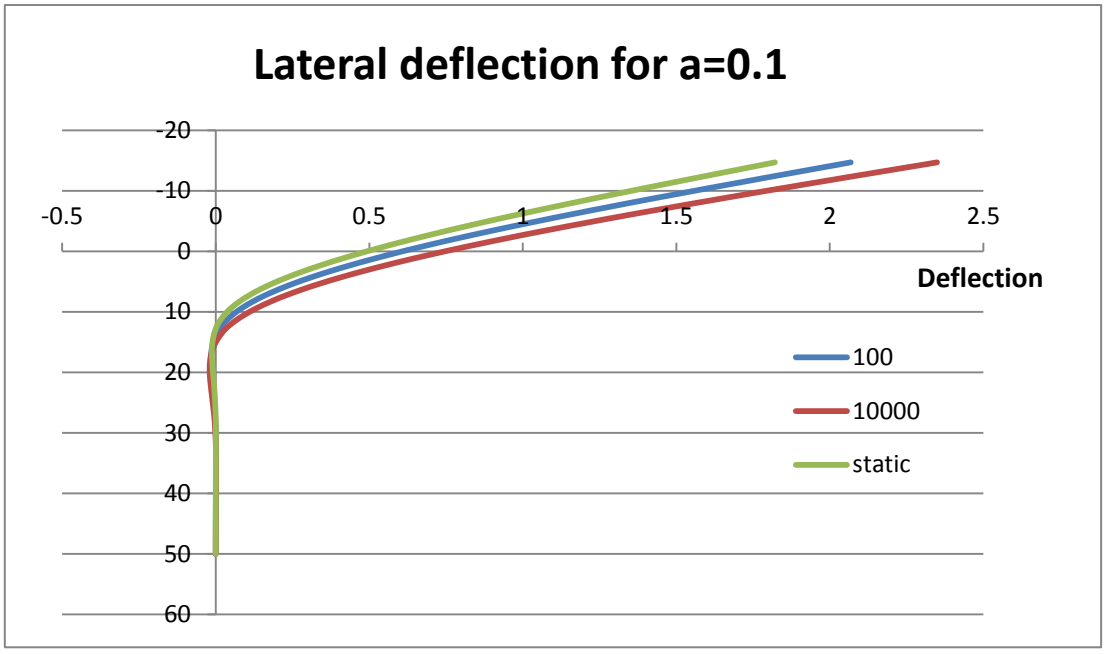

Figure 5-11 Later deflection for a=0.1

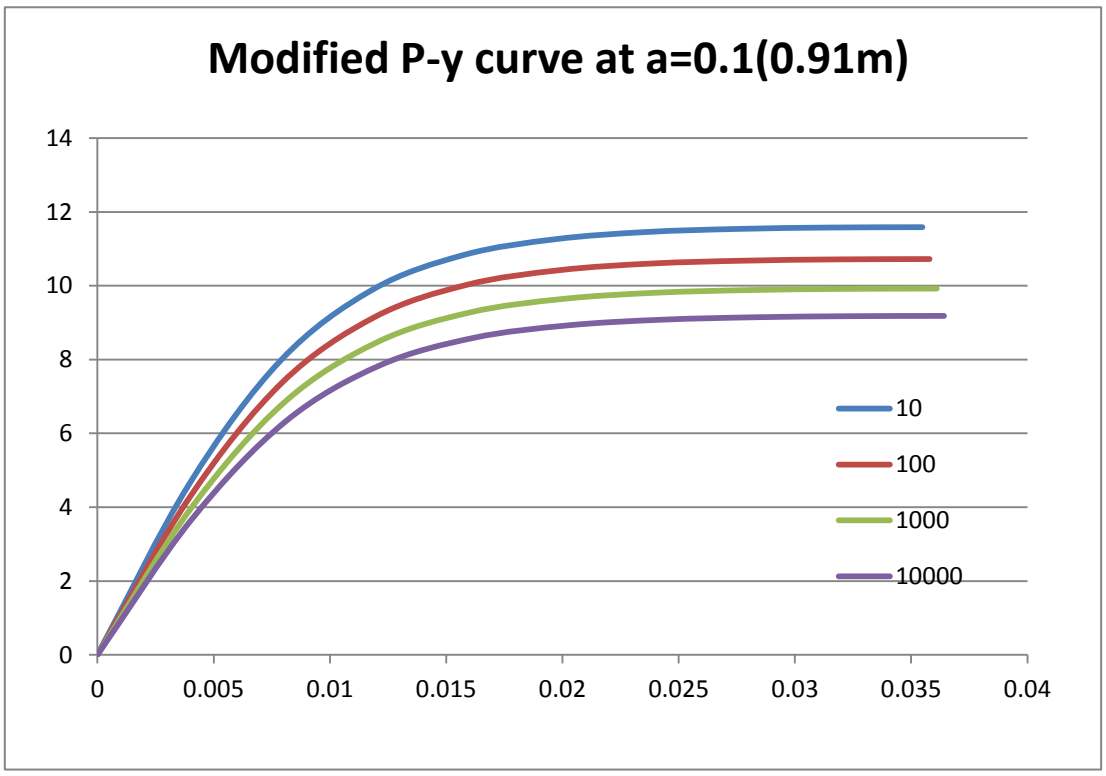

Figure 5-12 Modified P-y curve at a=0.1(0.91m)

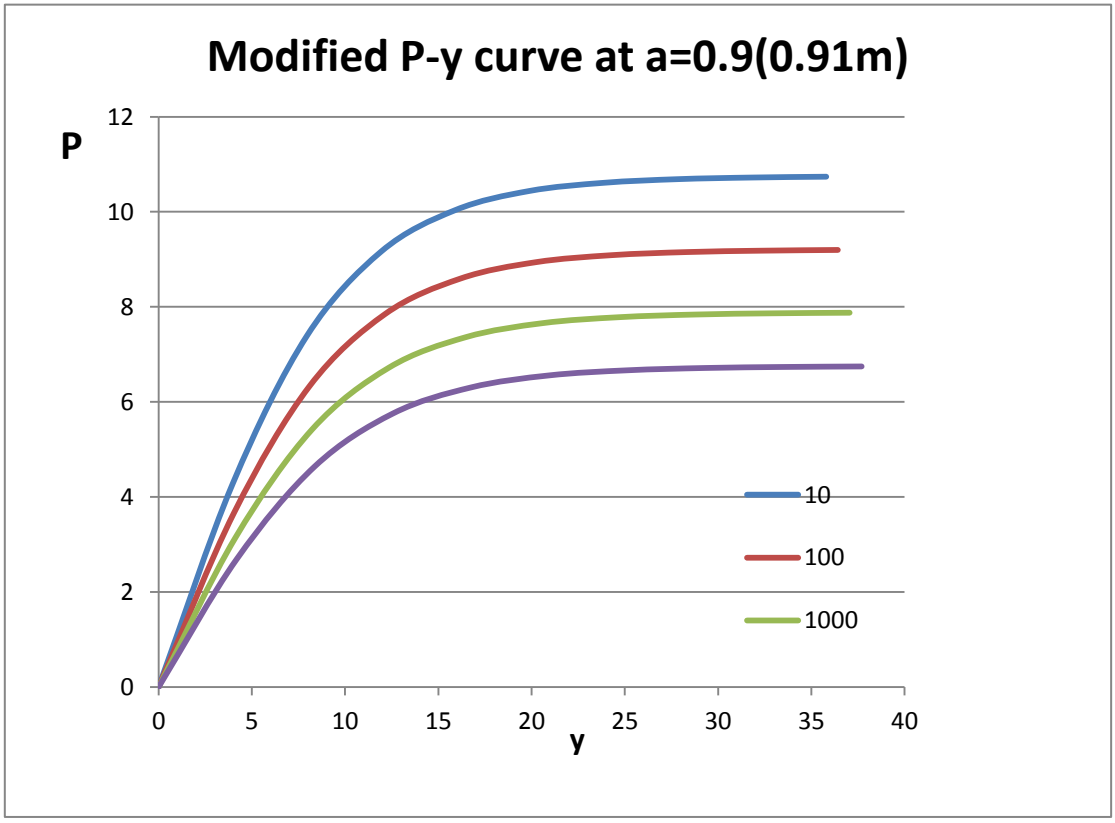

Figure 5-13 Modified P-y curve at a=0.9(0.91m)

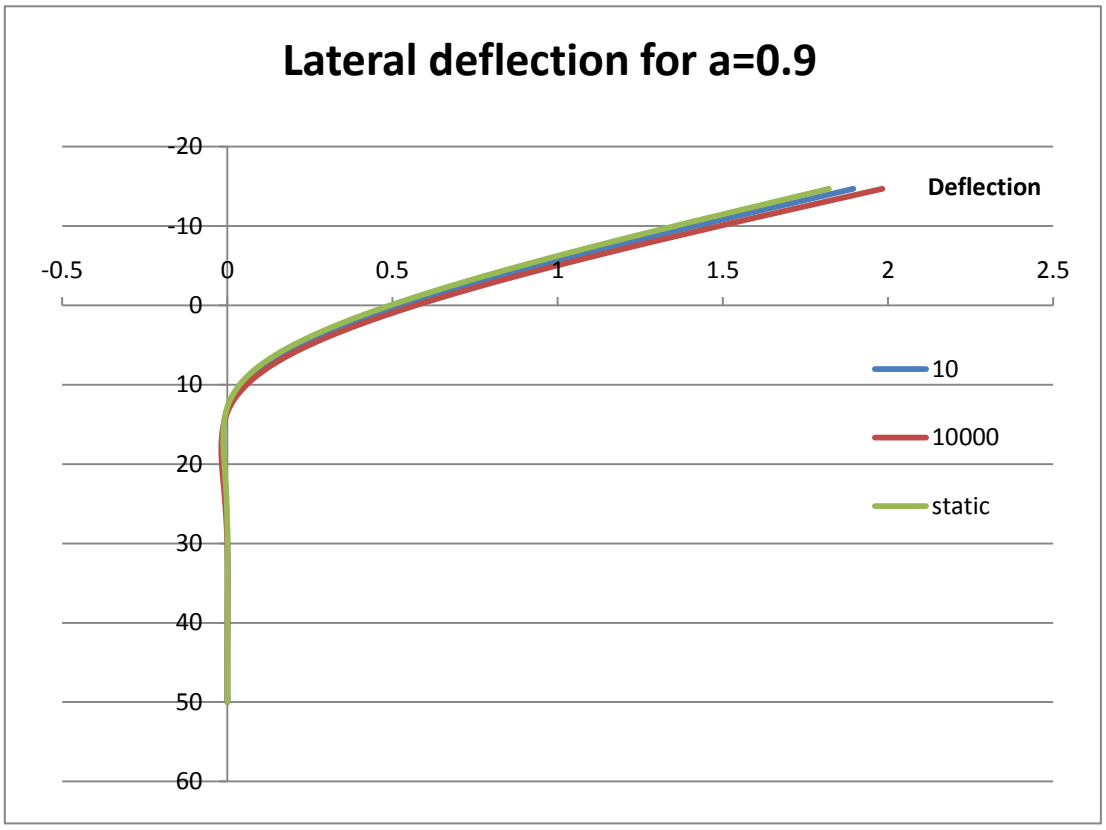

Figure 5-14 Later deflection for a=0.9

For the different value of correct factor a, it could obtain the relationship between correct factor and lateral deflection (Table 5-5). From the table, it's apparent that with the correct factor increasing, the lateral deflection at mud-line is decreasing, and also the deflection is most close to static loading deflection when correct factor a=0.9.

From the paper, the author recommended that theoretically, the value of a varies with depth, however, numerical investigations using a varying with depth provided no better agreement with the LISM method than with a constant value of 0.6. But for the different case, the value should be considered for the complicated conditions.

Table 5-5 Lateral deflections at mud-line for a=0.1, 0.6 and 0.9

Correct factor a	Lateral deflection at mud-line(10000 cycles)
0.1	72.01 cm
0.6	60.30 cm
0.9	54.70 cm
Static	51.4 cm

5.5.2.4 CYCLIC ANALYSIS FOR CASE 2 (H=9m, t=0.0748 and a=0.6)

In practical project, the height of BOP is range from 6m (250 tons) to 13m (450 tons), and the average height is chosen as 9m. The result of this case analysis will be more accuracy (Figure 5-15 and Figure 5-16).

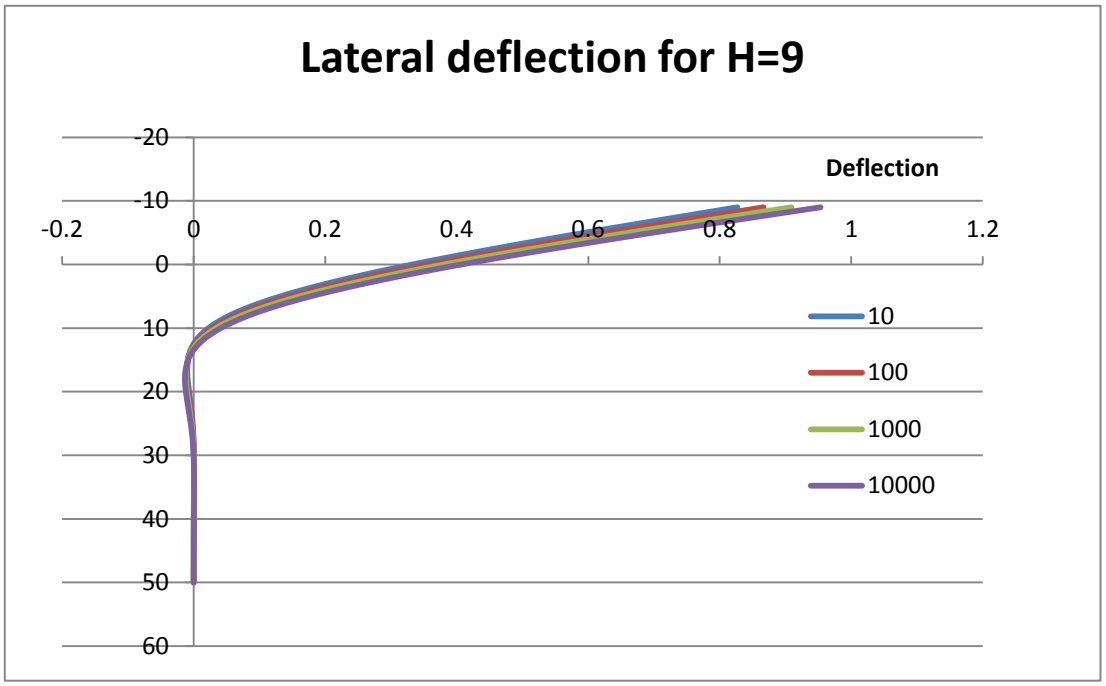

Figure 5-15 Lateral deflection for H=9

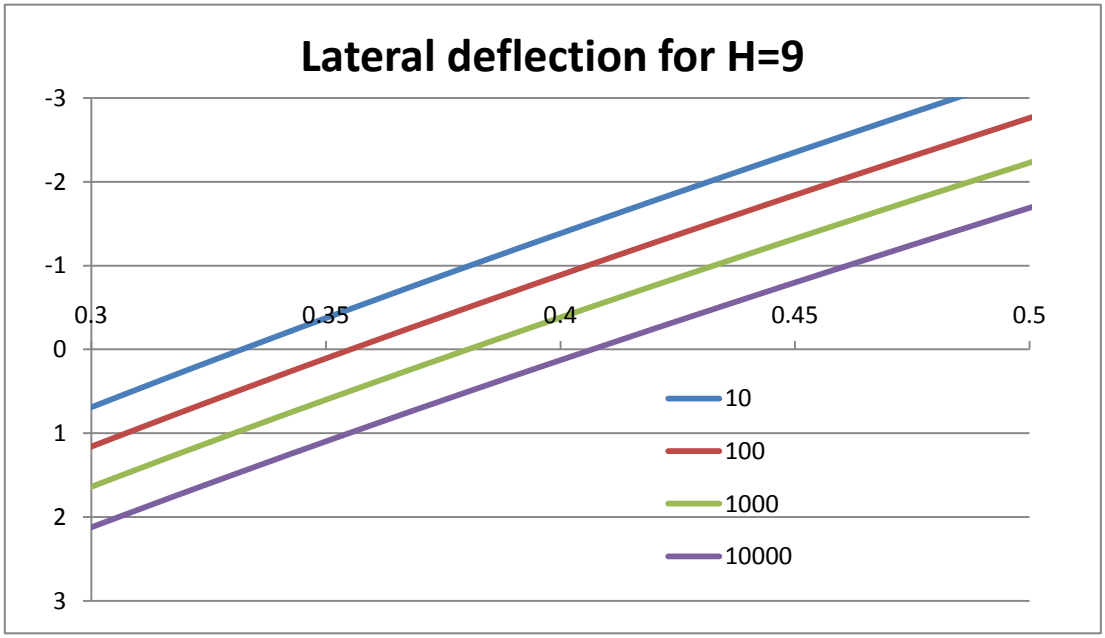

Figure 5-16 Lateral deflection for H=9

6 ANALYSIS AND CALCULATION USING MATLAB (BASIC THEORY OF LATERAL LOADED PILE)

In practical method, the reasonable results of lateral deflection of pile should include the nonlinear force-deformation property of soil. Moreover this property should combine with the elastic theory. From previous studies, actually the soil modulus constants are adjusted for each successive trial until satisfactory compatibility is obtained. In this paper, I introduce the nonlinear P-y curve with different depth. And also the basic differential equation and methods of computation (Lars Grande 1976, Ph.d. thesis) are given for elastic-pile theory. The analysis depends on the basic theory and I am programming on Matlab to calculate the lateral deflection of the conductor (Appendix A)

Due to introducing the nonlinear force-deformation property between conductor deflection and soil resistance, the elastic theory is used for several times, actually the calculation is performed on Matlab, I repeat to use P-y curve to get the rational solution (Figure 6-1) which means repeat until computed effective deflections consistent with assumed effective P-values.

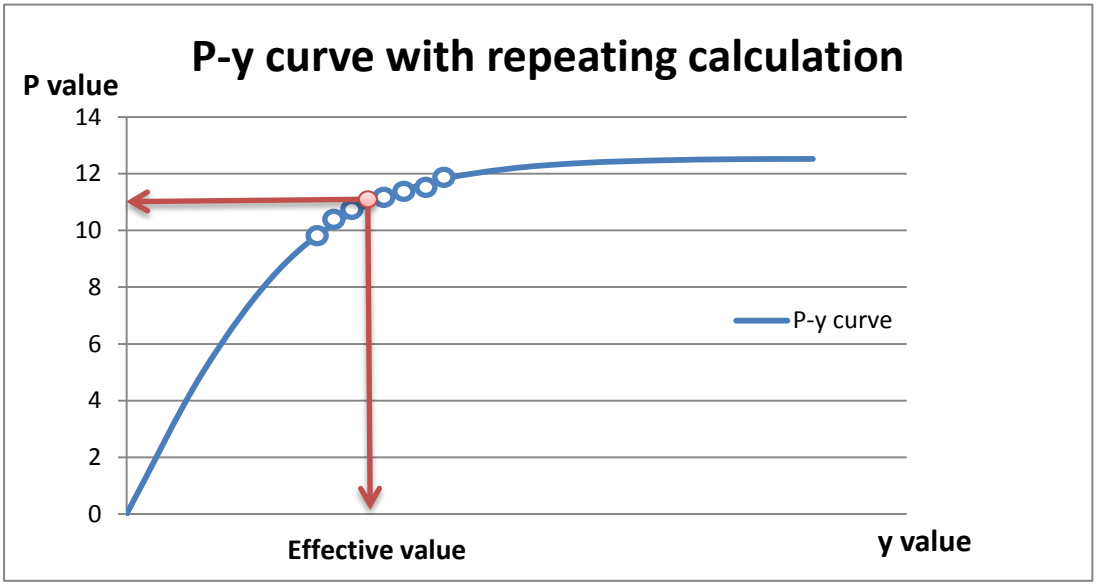

Figure 6-1 Loop calculation shown in P-y curve

For the P-y curve, in most cases, the soil modulus values tend to increase with depth. From the textbook we know that firstly soils frequently increase in strength characteristics with depth as the result of overburden pressures and of natural deposition, and secondly the deflection of conductor is decrease with the depth, where the soil modulus is defined as below:

$$E_s = \frac{-p}{y} \quad \text{.....Equation 6-1}$$

Where the negative sign indicates that the direction of the soil reaction is always opposite to the direction of conductor deflection, always the soil reaction is not a linear function of the pile deflection, and a typical nonlinear relation between p value and y value, see Figure 6-1.

In this topic, that the length of a conductor is 50m is considered for analysis, and the flexural stiffness EI is constant. The depth z, is measured downward from the seabed, therefore the boundary condition at the top contains an imposed moment and a shear force, see Figure 6-2. If the loads have different value, consequently the lateral displacement will be taken the different deflection pattern. With the P-y data applied, the different values of soil modulus will be obtained. Because of nonlinear P-y curve with depth influence, the soil modulus is a function of both z and y direction, therefore the form of the soil modulus with depth relationship also will change if the loading is changed.

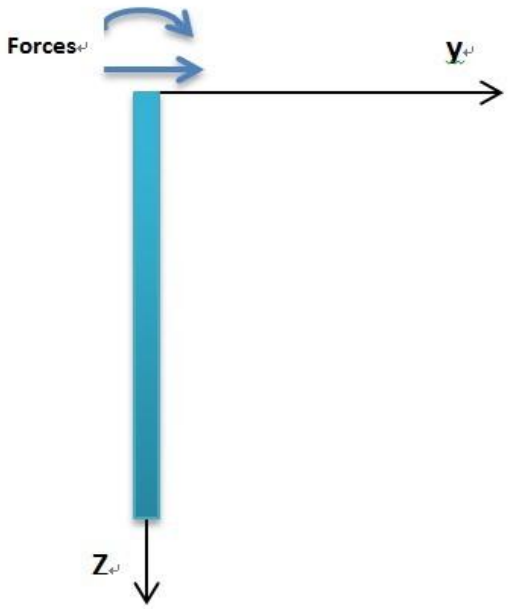

Figure 6-2 Conductor with forces

6.1 ELASTIC PILE THEORY

When the loading is applied on the conductor, the displacement consists of the conductor deflection and the elastic displacement of conductor. From the element which generally uses short elements near seabed and longer elements near pile tip, we can find the elements are laterally loaded soil resistance, P_r, which is proportional to lateral displacement in the same depth, in the meantime the up side and down side are loaded internal forces, see Figure 6-3.

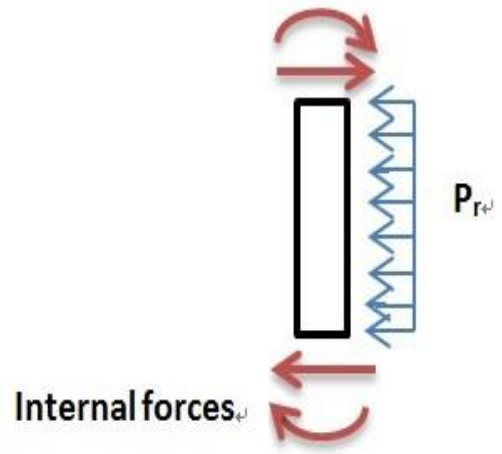

Figure 6-3 Conductor element with forces

If the conductor is considered as long pile, the length is not important for the analysis because the deflection of conductor at tip is approximate zero. And it needs to introduce some factor to express the lateral deflection of conductor:

$$y = f(z, T, L, E_s, EI, P_t, M_s) \quad \text{.....Equation 6-2}$$

Where:
T: Relative stiffness factor, as defined for each Es with different depth.
L: Length of conductor.
Es: Soil modulus.
EI: Flexural stiffness of conductor.
Pt: Shear force at conductor top (z=0).
Ms: Moment at conductor top (z=0).

Before the calculation and analysis, the assumption is introduced that the conductor is considered as elastic property and the lateral displacement is enough small, consequently it could use superposition theory for this topic, which means the deflection contain two parts: the first effect is deflection from shear force, Pt (y_1), and the other is introduced by moment, Ms (y_2).

If we analyze the problem separately as case1 and case2 (Matlock H, Reese LC 1960), the two conditions have two different functions of the same terms:

Case1: $\left[\frac{y1*EI}{P_t*T^3}, \frac{z}{T}, \frac{L}{T}, \frac{E_s*T^4}{EI}\right]$

Case2: $\left[\frac{y2*EI}{P_t*T^3}, \frac{z}{T}, \frac{L}{T}, \frac{E_s*T^4}{EI}\right]$

And also Matlock H and Reese LC suggested to satisfy conditions of similarity, each of the cases must be equal for both model or:

$$\frac{z_p}{T_p} = \frac{z_m}{T_m} \text{.....Equation 6-3}$$

$$\frac{L_p}{T_p} = \frac{L_m}{T_m} \text{.....Equation 6-4}$$

$$\frac{E_{s_p} * {T_p}^4}{EI_p} = \frac{E_{s_p} * {T_p}^4}{EI_p} \text{.....Equation 6-5}$$

$$\frac{y1_p * EI_p}{P_{t_p} * {T_p}^3} = \frac{y1_m * EI_m}{P_{t_m} * {T_m}^3} \text{.....Equation 6-6}$$

And

$$\frac{y2_p * EI_p}{P_{t_p} * {T_p}^3} = \frac{y2_m * EI_m}{P_{t_m} * {T_m}^3} \text{.....Equation 6-7}$$

So the deflection coefficient is:

$$C_{1y} = \frac{y_1 * EI}{P_t * T^3} \text{ for case1}$$

$$C_{2y} = \frac{y_2 * EI}{M_t * T^2} \text{ for case2}$$

From the deflection coefficient the deflection function could be shown as Equation 6-8:

$$y = \left[\frac{P_t * T^3}{EI}\right] C_{1y} + \left[\frac{M_t * T^2}{EI}\right] C_{2y} \text{.....Equation 6-8}$$

Due to obtaining a reasonable result, it still needs a specific set of case 1 and 2 coefficients which is function of the depth Z by a rationale model.

6.2 THE DIFFERENTIAL EQUATION OF SOIL-CONDUCTOR SYSTEM

The beam theory will be included, and the equation for the elastic beam is shown the equations below refer to Figure 6-3:

$$M = EI * y''$$

$$M' = Q$$

$$Q' = -P_r$$

By linear-elastic lateral conductor is lateral load Pr proportional to lateral displacement in this depth:

$$P_r = k_z * v$$

$$\frac{d^2v}{dz^2} = \frac{M}{EI} = \frac{d^2y}{dz^2} = y''$$

From the equation above,

$$v'''' + \frac{k_z * v}{EI} = 0 \text{.....Equation 6-9}$$

And boundary condition at top and tip are:

$$(1) z = 0, Q = Q_h; M = M_b$$

$$(2) z = L, Q = 0; M = 0$$

The Equation 6-9 can be solved analytically for constant reaction numbers, kz. The solution can be regarded as composed of boundary interference top to tip. The long flexible conductor disappear boundary disturbance from conductor tip. Conceivably impact composed of two cases charged moment (M_b), and lateral force charged (Q_h) conductor, each of reasonable easy for a long-flexible conductor and solution of Equation 6-9 found in the charts and tables in static and geotechnical engineering literature for different boundary conditions.

To solve the differential Equation 6-9, the derivative of the differential form is used below:

$$y_i'''' = \frac{1}{\Delta L_i}[y_{i+2} - 4 * y_{i+1} + 6 * y_i - 4 * y_{i-1} + y_{i-2}]$$

And on the differential form reads:

$$v_{i+2} - 4 * v_{i+1} + (6 + g_{yi}) * v_i - 4 * v_{i-1} + v_{i-2} = 0 \text{.....Equation 6-10}$$

Where:

$$g_{yi} = \frac{k_y * \Delta L^4}{EI}$$

$\Delta L = \frac{L}{n}$ and n is the numble of element of conductor.

The Equation 6-10 could be solved numerically using the Method Gleser developed lateral loaded pile (Lars Grande, Ph.d. thesis, 1976). The numerical solutions can be varied reaction number along the piles.

All in all, combination of the calculation above equations, we can do calculation on Matlab which should be a loop calculation, and the soil modulus is given by P-y data from result of SPLICE and Geosuite programs. The procedures of loop calculation are shown in Figure 6-4 and Figure 6-5, respectively.

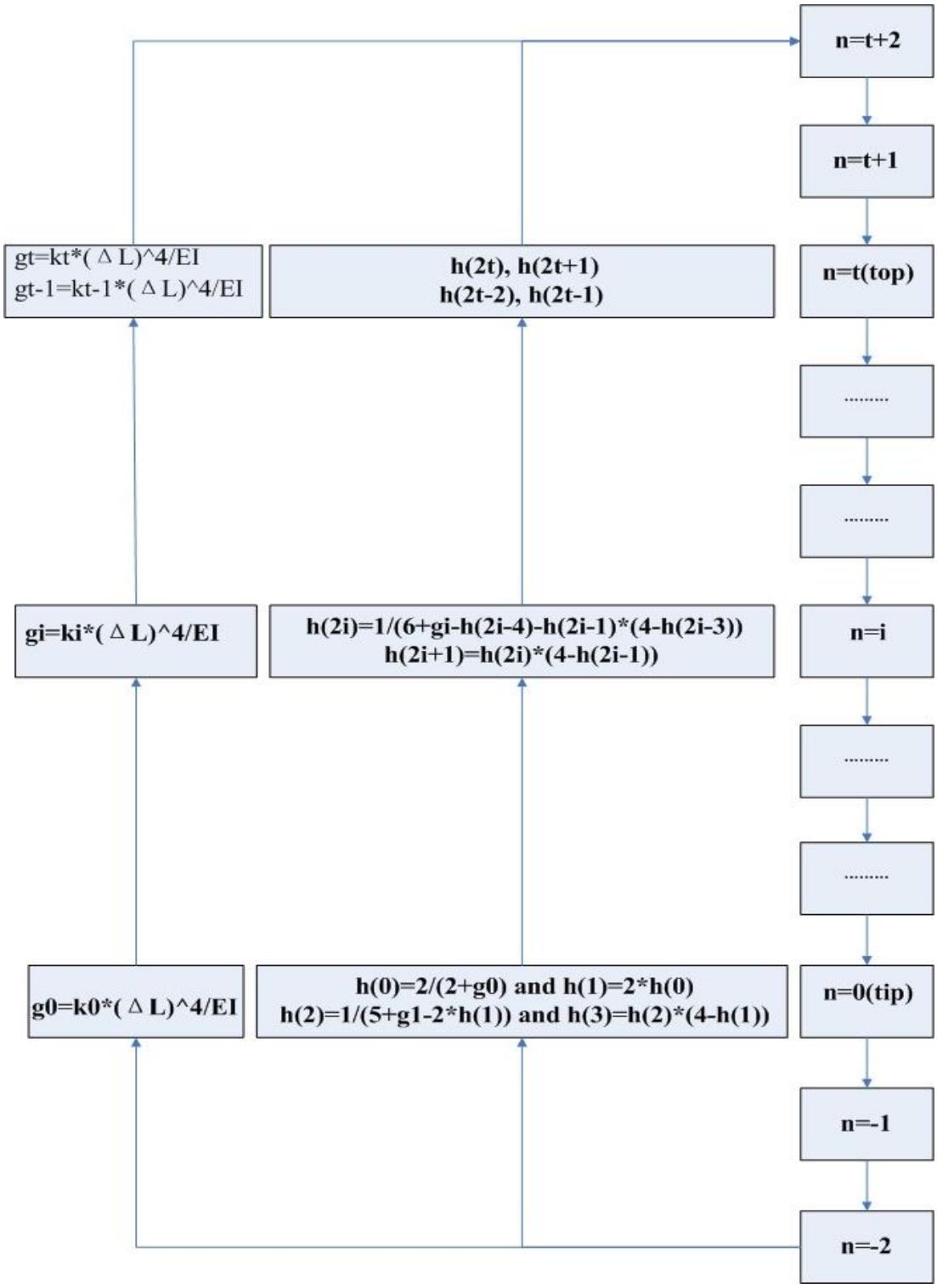

Figure 6-4 The h and g coefficients computation format along the conductor element

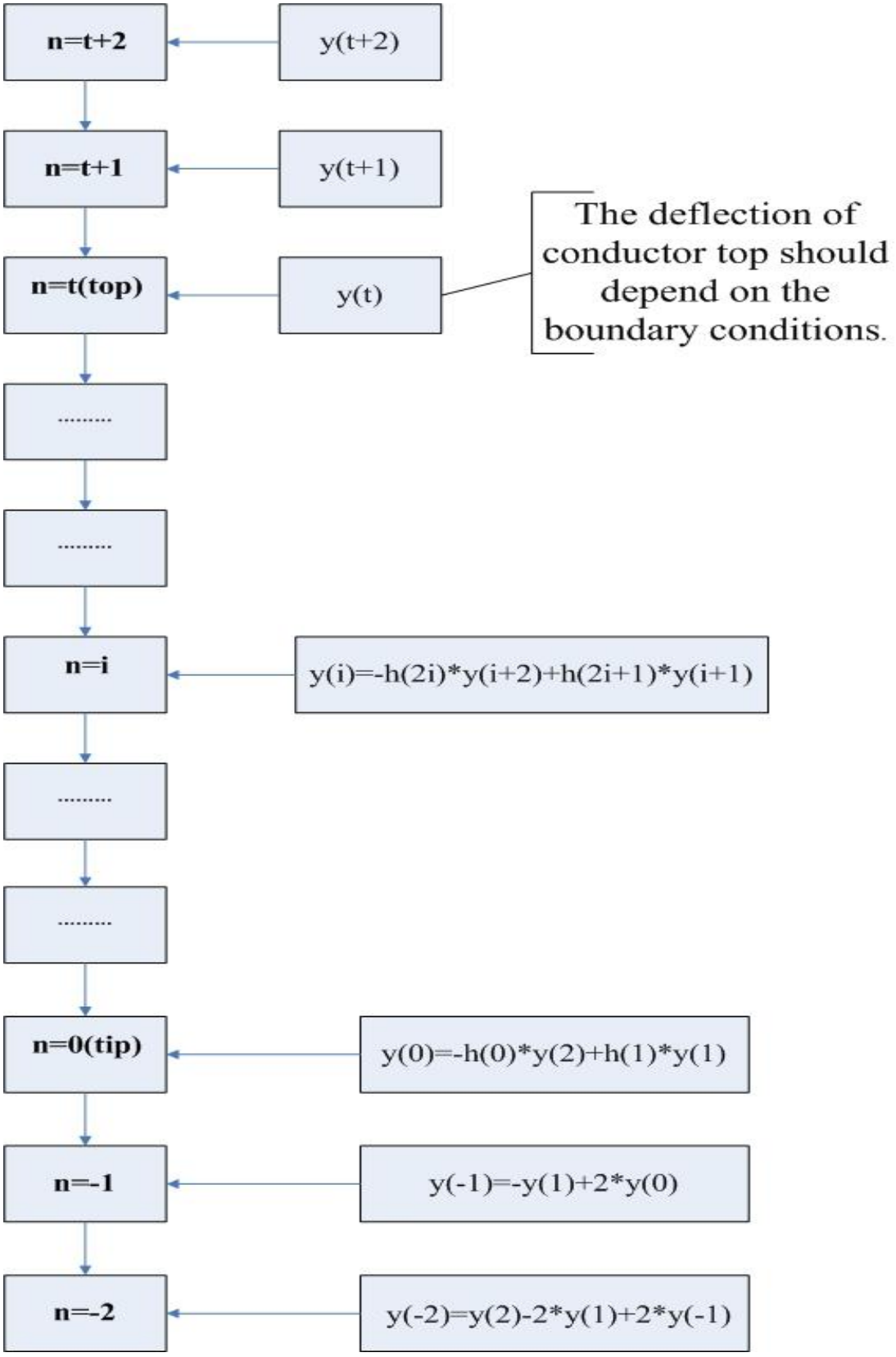

Figure 6-5 Deflection of conductor computation format along the conductor element

6.3 CALCULATION AND ANALYSIS IN MATLAB

6.3.1 ASSUMPTIONS IN CALCULATION

In this method, actually there are many factors which should be considered, however it mainly focus on the lateral deflection of elastic conductor and nonlinear P-y curve, and the difference from SPLICE calculation is that the gap between conductor and soil is included. There are assumptions for simplifying the case:

- The conductor fatigue problem and cement cracking in tension or compression are not included.
- The cyclic lateral loads are applied at the weight center of BOP and it is the two-way cyclic lateral load with same amplitude.
- The period of load is 10s, so this problem is cyclic analysis.

6.3.2 CONDUCTOR AND SOIL SYSTEM MODEL

Using the Matlab program and the P-y data from previous calculation, I will obtain the h and g coefficients in the difference-equation in the same model, see model Figure 5-1. In this calculation the two types of BOD is included:

- Weight of BOP=450 tons, and length of BOP=12m with 2000Kn horizontal force
- Weight of BOP=250 tons, and length of BOP=6m with 2000Kn horizontal force

The soil profiles and information of conductor are given by Table 5-1 and Figure 5-2, respectively. Moreover that the scour is considered in this calculation depends on the sediment transport theory.

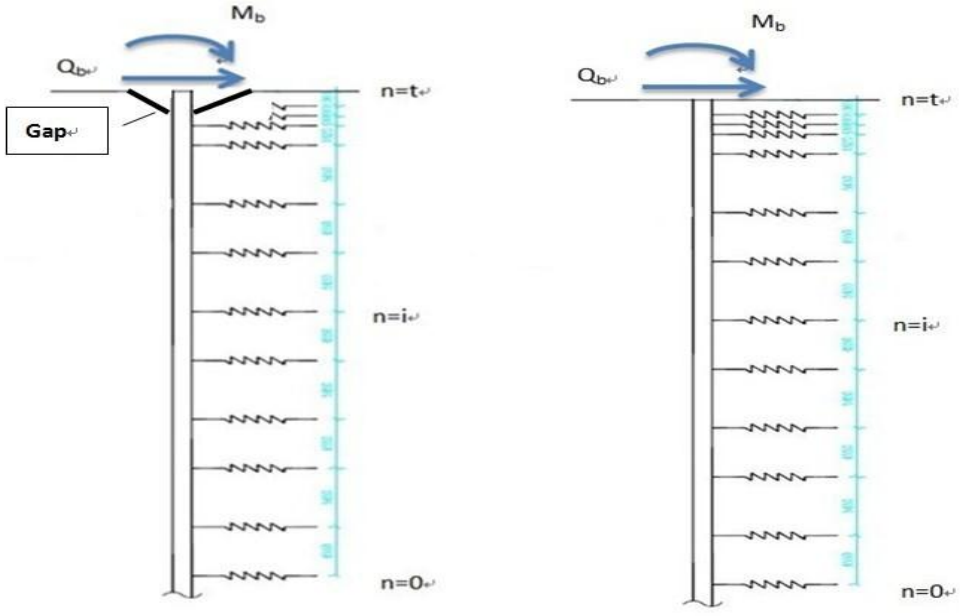

Figure 6-6 Soil and conductor system model with and without scour

6.3.3 SUMMARY AND RESULTS

With the stiffness of soil in static and cyclic obtained, the loop calculation on Matlab focus on checking the lateral deflection, and compare with the result in SPLICE. Moreover the data will also indicate the difference from the influence of gap. Therefore, there are 3 cases in this calculation:

- Case1: 2000Kn horizontal force, 450 tons BOP, with influence of gap.
- Case2: 2000Kn horizontal force, 450 tons BOP, without influence of gap.
- Case3: 2000Kn horizontal force, 250 tons BOP, with influence of gap.

In terms of modified P-y data in the calculation, the Equation (4-4 and 4-5) are operated with correct factor, **a** =0.6 which is suggested by (Long & Vanneste 1994), and degradation parameter, t=0.0748 which is conservative value that a mere 3% of the measure t values exceed the predicted valus.

Result for case1:

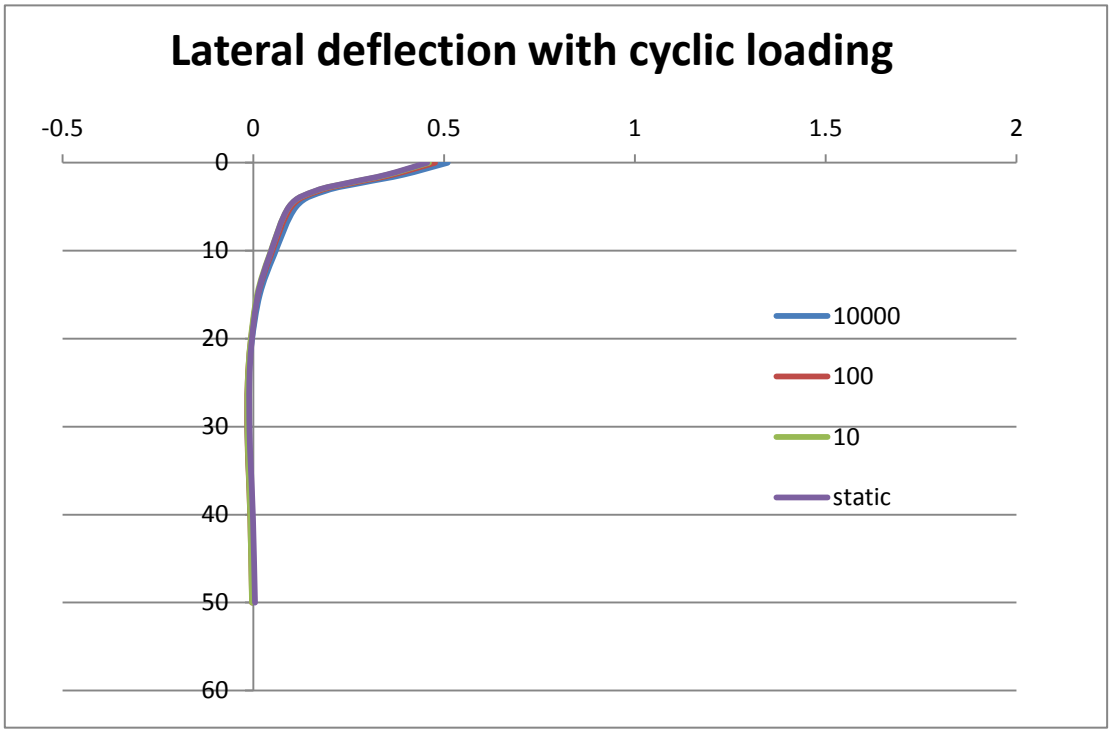

Figure 6-7-1 Cyclic loading lateral deflection for case1

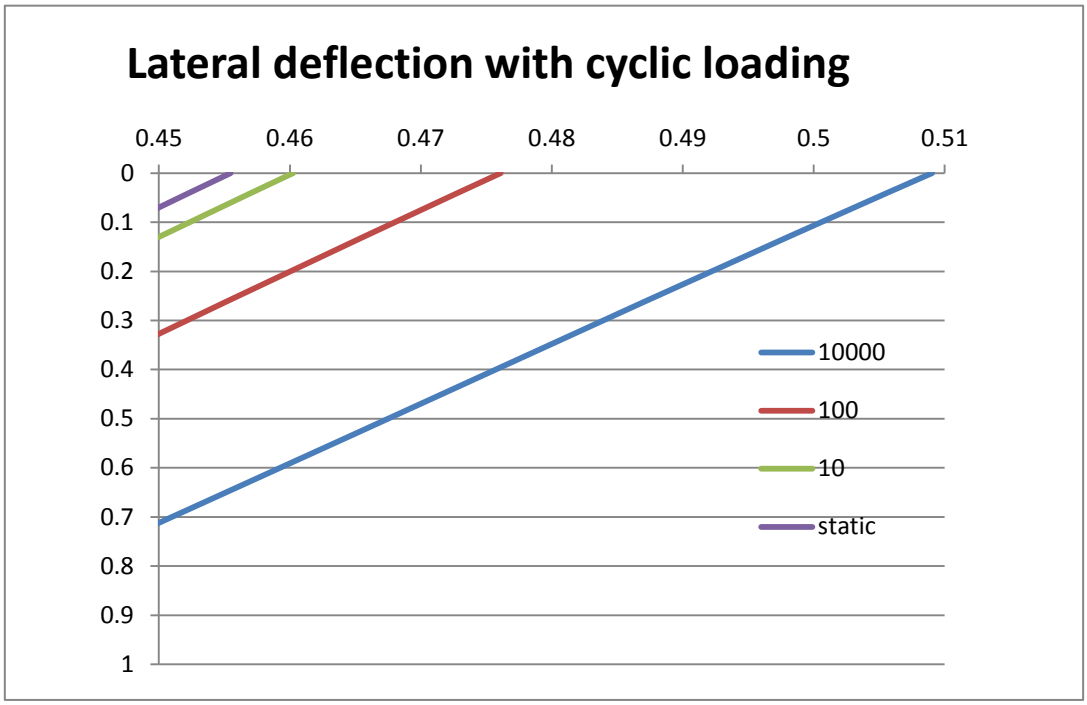

Figure 6-7-2 Cyclic loading lateral deflection for case1

Result for case2:

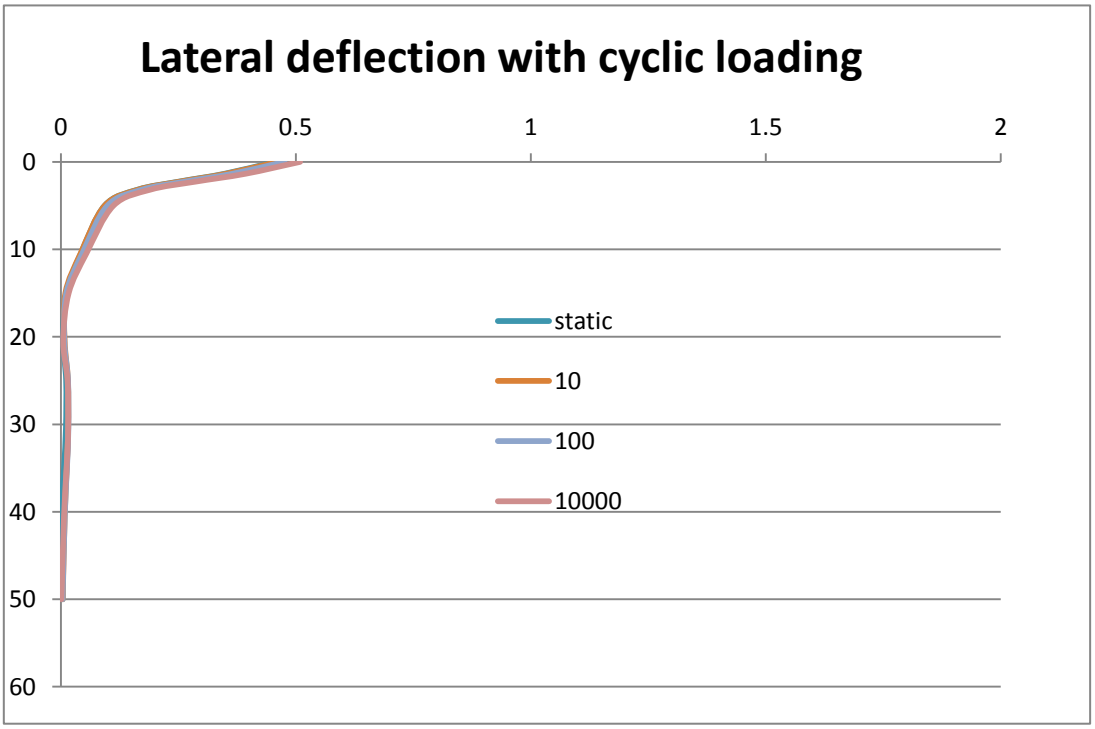

Figure 6-8-1 Cyclic loading lateral deflection for case2

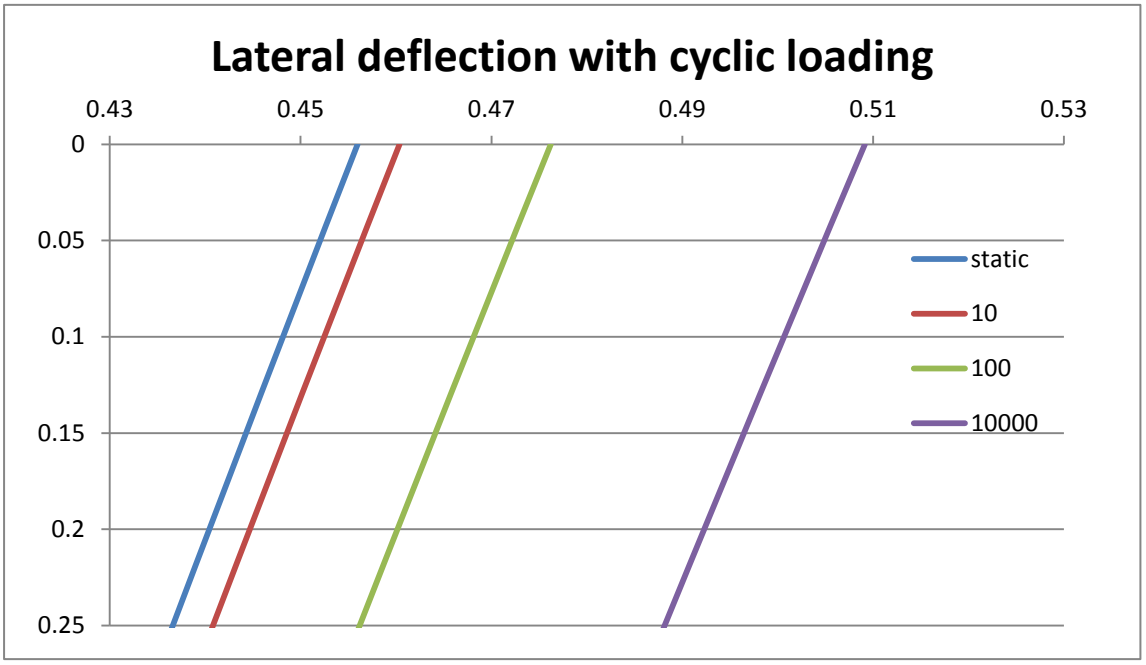

Figure 6-8-2 Cyclic loading lateral deflection for case2

Result for case3:

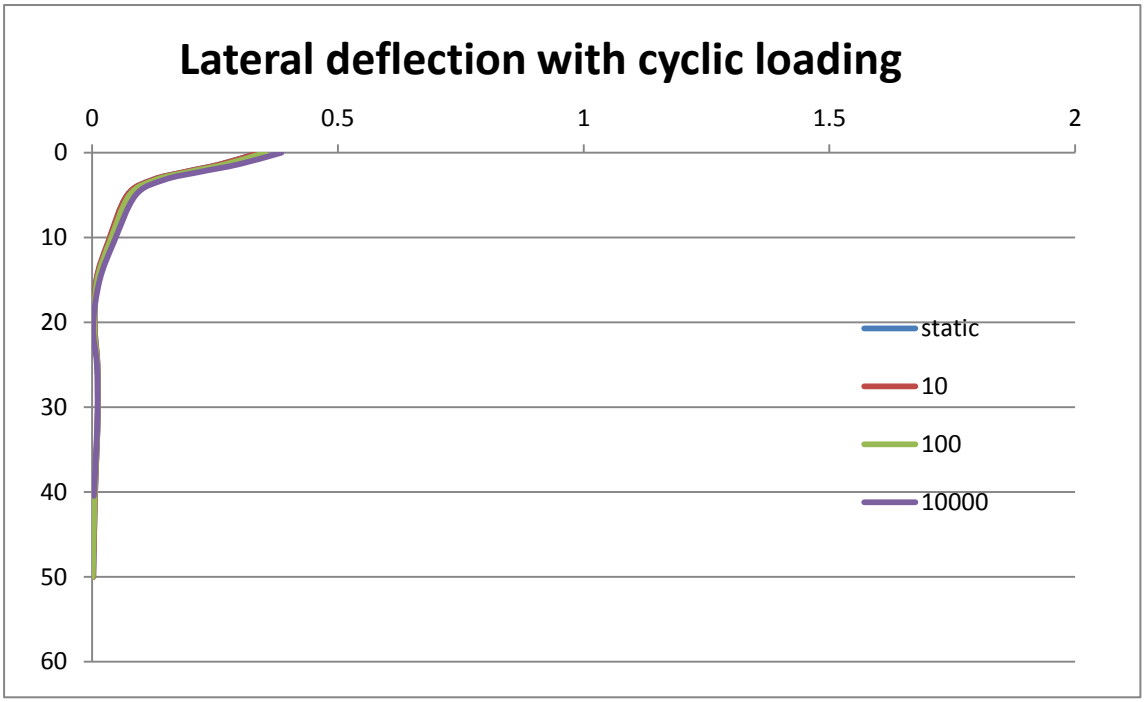

Figure 6-9-1 Cyclic loading lateral deflection for case3

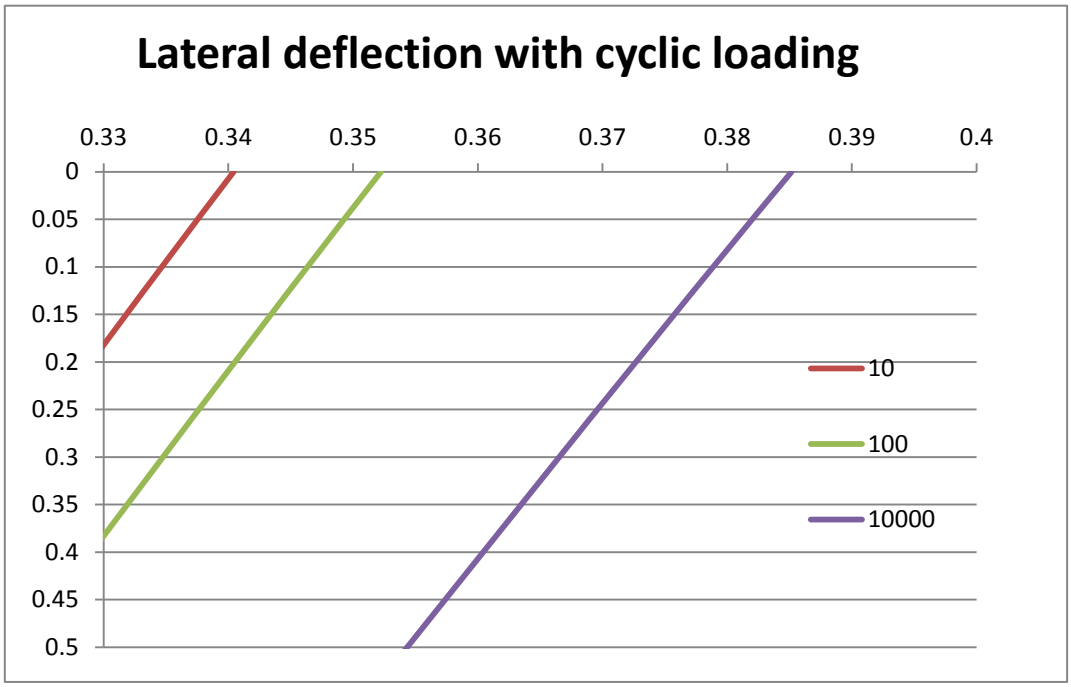

Figure 6-9-2 Cyclic loading lateral deflection for case3

Table 6-1 Summary the cyclic loading lateral deflection

Items	static	10 cyclic	100 cyclic	10000 cyclic
case1	0.455479	0.46025	0.476103	0.50904
case2	0.455971	0.460369	0.476224	0.509151
case3	0.336026	0.340424	0.352237	0.385164

The procedure of dynamic influence of conductor-soil system is that firstly the static deflection grows with increase of numble of cyclic loading, meanwhile the gap between soil and conductor is produced from Table 6-1 above, we can find that case2 with gap at 1.36 m below the seabed which gap have a influence on the deflection and the gap will deteriorate along the conductor with the increase of numble of cyclic loading. As can be found from this result, the deflection in case3 is less than that in case1and case2, which means that the weight of BOP has a dynamic influence on the deflection of system.

7 NATURAL FREQUENCY ANALYSIS

The natural frequencies of the conductor, BOP, wellhead and soil system have a significant influence on the system stability. The frequencies that correspond to the maxima magnification factor M which means the vibration could be

magnified. Without the damping impact, when a frequency of cyclic loads equal to the natural frequencies of the system, the magnification factor will be infinite, while the damping is included, the factor will also meet a peak value when the two kinds of frequencies meet each other, and which is defined as resonance, see Figure 7-1 below.

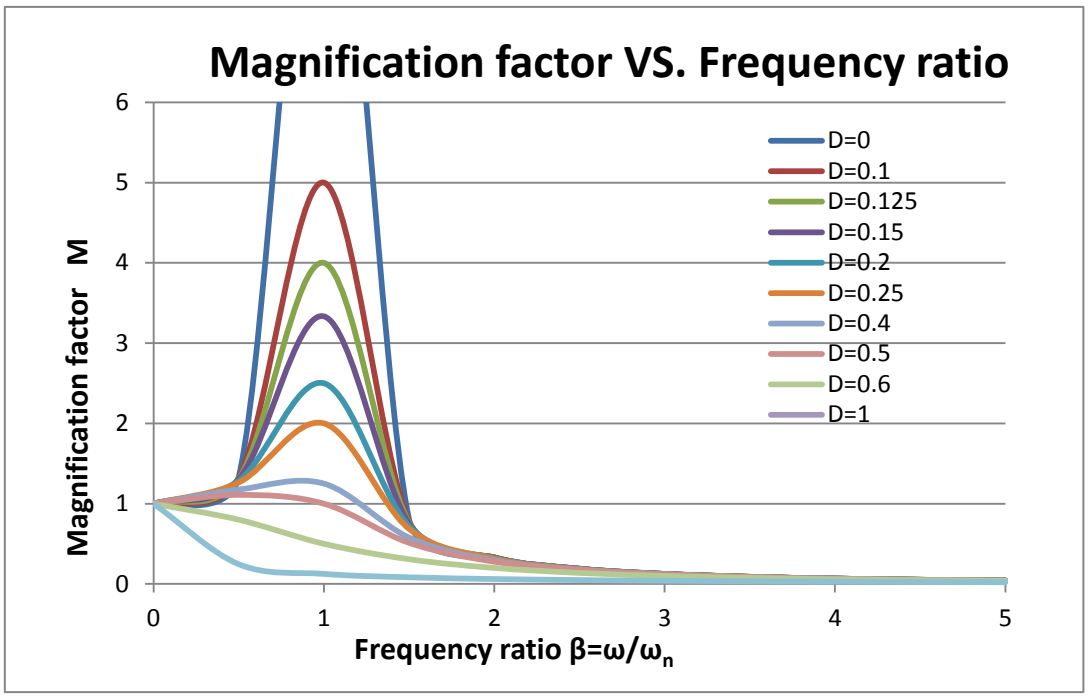

Figure 7-1 Magnification factor VS. Frequencies ratio at different damping ratio.

In practical project, the resonance condition is very dangerous for the system, consequently the natural frequency analysis should be performed and will give a strong support for designing work.

7.1 BASIC THEORY OF NATURAL FREQUENCY

In single-degree-of-freedom system, see Figure 7-2, mass-spring-damper system, the natural frequency is related to the mass and stiffness of system (Equation 7-1 and Equation 7-2).

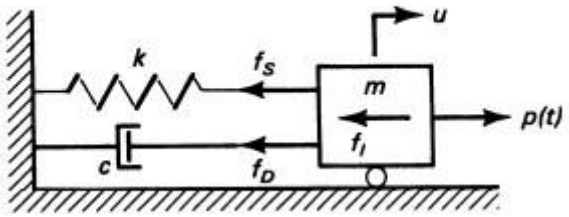

Figure 7-2 Single-degree-of-freedom system

$$\omega_n = \sqrt{\frac{K}{M}} \text{.....(Equation 7-1)}$$

$$m\ddot{v} + kv = 0 \text{ .....(Equation 7-2)}$$

From the equation, it could be found the natural frequency is a property of the whole system and the term natural is used to describe each of these vibration properties to emphasize the fact that these are natural properties of the system, therefore, that is not changed with the variation of cyclic loading.

Nowadays, in the complicated practical engineering analysis, the several-degree-of-freedom system is always used in projects, and the multiple-degree-of freedom model could be more accurate to describe the practical system than single DOF, see Figure 7-4.

Due to the multiple-degree-of freedom problem, the eigenvalue problem whose solution gives the natural frequencies and modes of a system which does not fix the absolute amplitude of the vectors, only the shape of the vector given by the relative values of the N displacements. Moreover, corresponding to the relative values of the N natural vibration frequencies ω_n of an N-DOF system, there are N independent vectors, natural modes of vibration ($\emptyset_n$), which contribute the deflection of the system by different weight, it will be introduced lately.

As we known that the natural frequency is the property of the dynamic system, the model with free vibration and without any dynamic excitation external forces or support motion could be clear to introduce the property. The model may be expressed for this case as:

$$\mathbf{m\ddot{u} + ku = 0} \text{.....Equation 7-3}$$

And the displacement can be known as:

$$\mathbf{u}(t) = \emptyset_n(A_n cos\omega_n t + B_n sin\omega_n t) \text{ .....Equation 7-4}$$

Where A_n and B_n are constants of integration that can be determined from the initial conditions that initiate the motion and $\mathbf{u}(t)$ is the deflection vector. Substituting this form of $\mathbf{u}(t)$ in Equation 7-3 gives:

$$[\mathbf{k} - \omega_n^2 * \mathbf{m}]\emptyset_n = \mathbf{0} \text{.....Equation 7-5}$$

From the Equation 7-5, which can be interpreted as a set of N homogeneous algebraic equations for the N elements $\emptyset_{in}$ (i=1,2,3,4,...,N). This set always has the trivial solution$\emptyset_n$=0, however the solution is helpless for the analysis because it means that the motion of the system is zero, therefore, there is no

trivial solution in the equation, when:

$$\det[\mathbf{k} - \omega_n^2 * \mathbf{m}] = \mathbf{0} \quad \text{.....Equation 7-6}$$

Where:
k: is the stiffness matrix of the system which combines of stiffness of conductor and springs.
m: is mass matrix of the system which includes mass of conductor and BOP.
$\emptyset_n$: is shape of the vector given by the relative values of the N displacements.

Resolving the problem, a polynomial of order N in ω_n^2 is obtained; meanwhile the Equation 7-6 is named as frequency equation. This equation has N real and positive roots for ω_n^2 because the mass and stiffness of system are symmetric and positive definite, furthermore, with the conductor assumed as elastic pile, the positive definite property of k matrix is assured for that prevents rigid-body motion. In the meantime the positive feature of m matrix is also assured for that the mass of system is nonzero and positive.

With result of the problem, there are N natural frequencies ω_n is determined which are defined as eigenvalues or characteristic values. Each natural frequency substitute into the Equation 7-5, then the corresponding vector $\emptyset_n$ could be obtained which do not determine the absolute amplitude of the vectors, just the shape of the vector given by the relative values of the N displacements.

Overall the multiple-degree-of freedom system has N natural vibration frequencies ω_n (n=1, 2, 3… N) which will be arranged in sequence from smallest to largest, and the smallest frequency is named first or fundamental frequency.

7.2 NATURAL FREQUENCY ANALYSIS OF THE BOP WITH CONDUCTOR –SOIL SYSTEM

The multiple-degree-of freedom model is operated in this case, therefore, the conductor is considered as an elastic pile which is divided into several elements, and the conductor only connect soil with springs, meanwhile the BOP is allocated at top of the conductor as a mass. In practical, the weights of BOP are 450 tons and 250 tons and the length between wellhead to seabed is approximate 3 meters. The wind, waves and other cyclic loading are random loading, consequently 2000kN will be supposed as average cyclic loadings to operate on the BOP, which will demonstrate the natural frequencies of system with soil spring stiffness (see Figure 7-3).

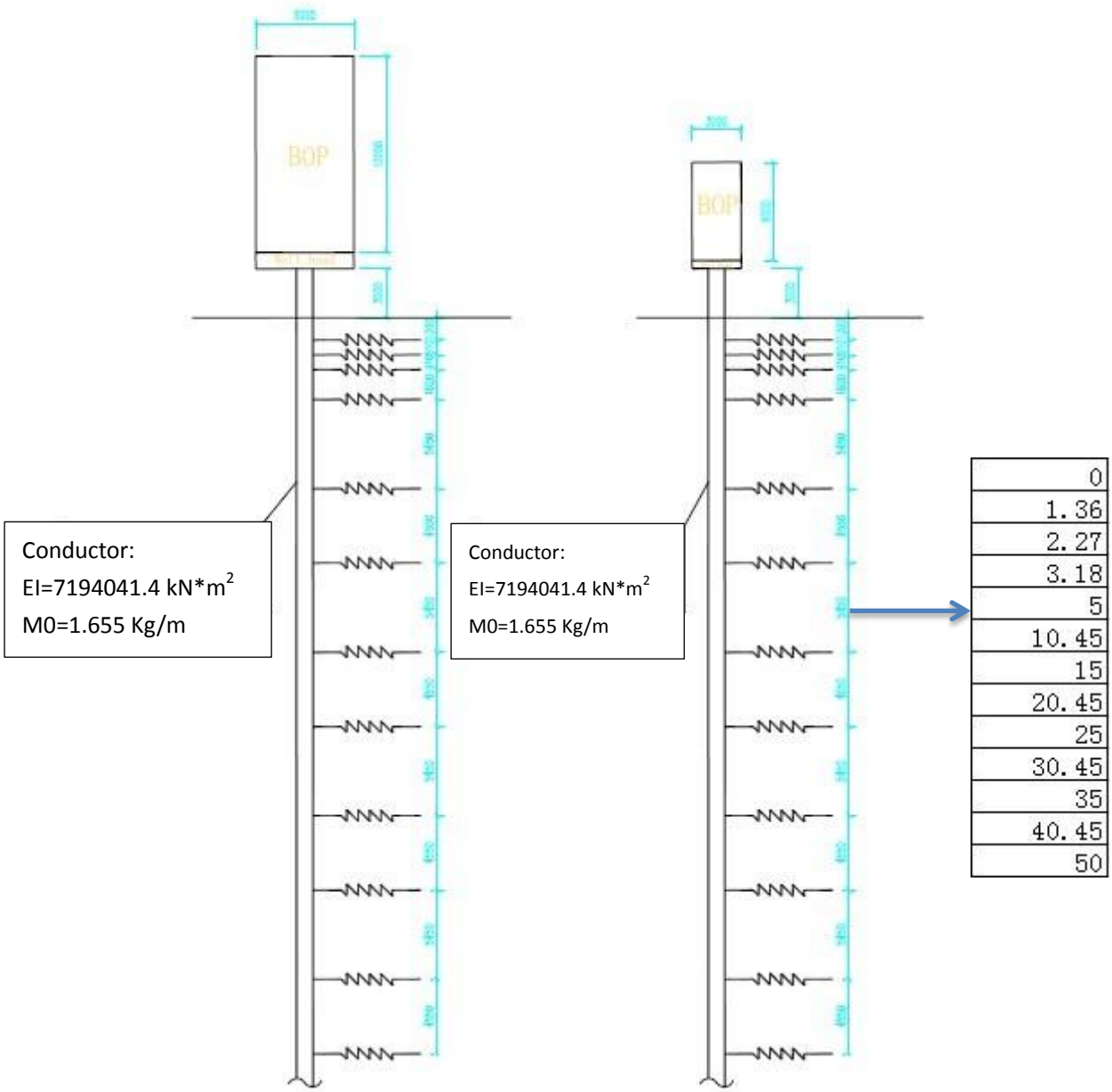

Figure 7-3 Two models of the natural frequency analysis

7.2.1 NATURAL FREQUENCY ANALYSIS

7.2.1.1 INTRODUCTION OF MODEL

In general, a node in a planar two-dimensional frame has three DOFs--two translations and one rotation (Figure 7-4). The DOFs arrange from the bottom of BOP to the tip of the conductor, and each node connects to the spring, so there are 28 DOFs in the case.

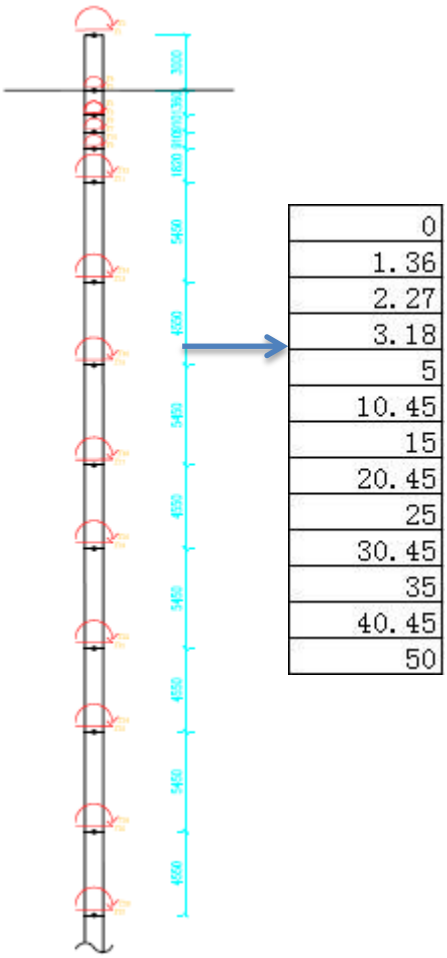

Figure 7-4 MDOF model for analysis

These cases focus on the lateral displacement of the conductor so that the axial deformations in any of the system can be neglected. In each node, there are two DOFs, lateral translations and rotation. However, the BOP is needed to transfer the mass from the local axes to global axes, see Figure 7-5 below, and the Equation 7-6 is used below.

7.2.1.2 CALCULATION OF NATURAL FREQUENCY

First of all, the mass and stiffness matrix should be calculated including the BOP and conductor. The BOP is considered as the rigid body, while the conductor is suggested as the flexible, as a result, the mass matrix should including the influence of BOP, and meanwhile the stiffness would consist of soil stiffness and flexible stiffness of conductor. With the constant average mass of conductor assumed, the consistent element matrix for plane frame element method (Appendix C) is used in this calculation for both mass and stiffness matrices.

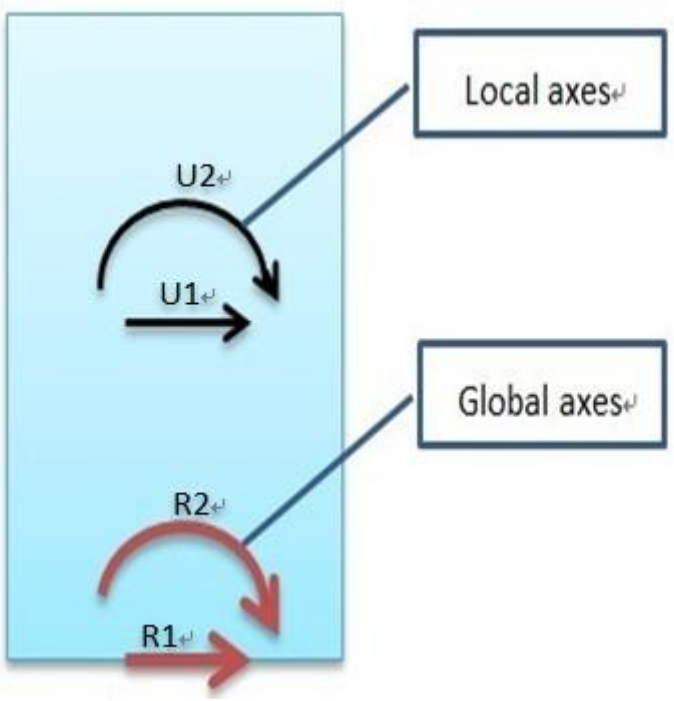

Figure 7-5 Local axes and Global axes for BOP

$$\mathbf{U} = \begin{Bmatrix} \mathbf{U_1} \\ \mathbf{U_2} \end{Bmatrix} = \begin{bmatrix} \mathbf{1} & -\frac{\mathbf{L}}{\mathbf{2}} \\ \mathbf{0} & \mathbf{1} \end{bmatrix} \begin{Bmatrix} \mathbf{R_1} \\ \mathbf{R_2} \end{Bmatrix} = \mathbf{A} * \mathbf{R} \quad \text{.....Equation 7-7}$$

And virtual work theory is performed as:
The work done should be the same

$$\boldsymbol{\delta}\mathbf{U}^{\mathbf{T}}(\mathbf{M_{local}} * \ddot{\mathbf{U}}) = \boldsymbol{\delta}\mathbf{R}^{\mathbf{T}}(\mathbf{M}_{\text{global}} - \ddot{\mathbf{R}}) \text{.....Equation 7-8}$$

And then substitute Equation 7 into Equation 8:

$$\mathbf{A}^{\mathbf{T}} * \mathbf{M_{local}} * \mathbf{A} = \mathbf{M_{global}} \text{.....Equation 7-9}$$

Where:
δU: The virtual displacement vector in local axes.
M_{local}: Mass matrix for first and second DOF in local axes.

M_{global}: Mass matrix for first and second DOF in global axes.

A: Transfer matrix from local axes to global.

Then, the mass matrix need to include the influence of water. The added mass is the mass of water displaced by the submerged elements. Contained mass is the water contained or enclosed by the submerged elements that are flooded. The added mass is taken as the mass of the water displaced by the submerged part of members. The contribution of added mass due to the increased member diameter caused by marine growth is included.

The added mass M is based on the following expression below:

$$M = \frac{C_m * \rho_{water} * \pi * d^2}{4}$$

Where:
C_m: Coefficient of mass.
ρ_{water}: Density of water.
d: Diameter of element (including marine growth).

Then the global stiffness matrix will be obtained when the BOP is treated as rigid. And substitute the global stiffness and mass matrix into Equation 7-6. The eigenvalue problem in this paper will be resolved in Matlab.

7.2.1.3 SUMMARY AND ANALYSIS

It depends on the model in Figure 7-4, there are 6 cases in the calculation:

- Case1:450 tons BOP, without scour.
- Case2:450 tons BOP +water influence (50% total weight of BOP), without scour.
- Case3:450 tons BOP, with scour.
- Case4: 450 tons BOP +water influence (50% total weight of BOP), with scour.
- Case5: 250 tons with scour.
- Case6: 250 tons BOP +water influence (50% total weight of BOP), with scour.

From case1 to case4, the results indicate the influence of scour which means that with increasing numble of cyclic loading the gap between soil and conductor is extending and the natural frequencies of system also will change, therefore the calculation will reduce the top two springs from the seabed to simulate the influence of scour. The case5 and case6 demonstrate that the different weight of BOP should introduce the different natural frequencies for system.

Table 7-1 The Natural frequencies with static loading

	1st Frequency	2ed Frequency	3rd Frequency
case 1	0.4417405 Hz	2.037127 Hz	4.189621 Hz
case 2	0.3675488 Hz	1.820963 Hz	3.926536 Hz
case 3	0.4428411 Hz	2.040032 Hz	4.190729 Hz
case 4	0.3684254 Hz	1.823241 Hz	3.928688 Hz
case 5	0.5913135 Hz	3.104924 Hz	6.149235 Hz
case 6	0.5007694 Hz	2.975663 Hz	5.587625 Hz

From the Table 7-1, the static natural frequencies analysis indicates that the weight of BOP have an important influence on natural frequencies of system, with the weight of BOP increasing, the first frequency value is decrease, and from the calculation, it can be concluded that if the weight of BOP is increasing and much larger than the weight of conductor, so the second natural frequency is closed to fundamental frequency in the system and vice versa.

Table 7-2 The Natural frequencies with cyclic loading (100 cyclic)

	1st Frequency	2ed Frequency	3rd Frequency
case 1	0.4261325 Hz	2.022414 Hz	4.179282 Hz
case 2	0.3547801 Hz	1.807742 Hz	3.914816 Hz
case 3	0.4239041 Hz	2.021371 Hz	4.178725 Hz
case 4	0.3529433 Hz	1.806624 Hz	3.914488 Hz

After 100 cyclic loading the values in Table 7-2 compare with static condition in Table 7-1, when the gap start to extend and soil degradation is included, the cyclic loading decrease the stiffness of soil meanwhile the natural frequencies is lower than that in static loading. When the system suffers cyclic loading continuously, it is apparent that the soil is weaker than before and natural frequencies of system continuously drop down, and the decrease is significant in first frequency after 10000 cyclic loading, see Table 7-3.

From the calculation, the accuracy of the natural frequency analysis depends on numble of element of conductor, which means the more elements chosen, the more accuracy in the results. However the high numble of elements will make calculation slowly.

Table 7-3 The Natural frequencies with cyclic loading (10000 cyclic)

	1st Frequency	2ed Frequency	3rd Frequency
case 1	0.4088524 Hz	2.010737 Hz	4.172923 Hz
case 2	0.3405782 Hz	1.796507 Hz	3.908818 Hz
case 3	0.4068188 Hz	2.009862 Hz	4.172439 Hz
case 4	0.3388997 Hz	1.795561 Hz	3.90854 Hz

8 CONCLUSIONS

In one part this master thesis, the basic cyclic analysis and soil degradation are introduced. The theoretical knowledge suggests the correct method for cyclic loading applied on the conductor, and check the method used in this problem. In this case the nonlinear springs is arranged below the mud-line which indicates that the nonlinear behavior of soil and the stiffness of soil could be changed by cyclic loading and different depth. The DSPY(Deterioration of Static P-y Curve) method and API 1987 code are operated in the project for cyclic loading and static loading, respectively. The DSPY method deteriorates the resistance supported by a static P-y curve to account for the effects of cyclic lateral loads, and then the modified P-y curve will describe the influence of cyclic loading.

Furthermore, the effect of degradation parameter t, correct factor **a** and height of BOP are included in the paper. From previous method and tests, a=0.6 is recommended to use in practical project and there are some more factors influence on degradation parameter t, such as effect of depth coefficient, soil density, installation method and cyclic load ratio. With the t increasing, the soil degradation is more deteriorative. However degradation parameter t is totally difficult to determine which is caused by a lot of practical factor affecting the value of t. And also correct factor **a** is arranged from 0 (P value changed only) to 1 (y value changed only). However, the method proposed is an empirical approach intended to provide the designer with a simple and expedient means to estimate effects of cyclic lateral load on piles in sand. Because of the empirical methods, so it needs to continue to include more parameters and results of field and lab tests to verify or modify the recommendations.

In this thesis, the correct factor a=0.1, 0.6 and 0.9 are performed for calculation, and it is apparent that the deflection is most closed to static loading deflection when correct factor a=0.9, in the meantime, the value equal to 0.6 is recommended. In the chapter 6, all the calculation depends on the modified P-y data with correct factor a=0.6, meanwhile, we can find influence of the scour around conductor with different cyclic loading applied on BOP. All in all, after 10000 cyclic, the soil degradation is significant, and deflection is apparently increasing. During the cyclic loading applying, the gap between soil and conductor is also produced, and the gap make less soil resistance near the seabed, consequently the deflection should be more than before, but the influence is not significant at 10, 100 and 1000 cyclic.

The natural frequencies of the conductor, BOP, wellhead and soil system have a significant influence on the system stability. The frequencies that correspond to the maxima magnification factor M which means the vibration could be magnified. Without the damping impact, when a frequency of cyclic loads

equal to the natural frequencies of the system, the magnification factor will be infinite, while the damping is included, the factor will also meet a peak value when the two kinds of frequencies meet each other. In this paper, the results of calculation indicate the natural frequencies of two types of BOP (250 tons and 450 tons) with cyclic influence. Actually the change of the fundamental frequency is also not significant at 10, 100 and 1000 cyclic, but at 10000 cyclic.

Overall the cyclic loading (waves, wind and ocean) have an important influence on the stability of offshore structure, when the foundation is designed, the dynamic analysis should be done.

9 RECOMMENDS AND FURTHER WORK

Actually the problems of cyclic loading and soil degradation are simplified and some important factors like plastic deformation zone, fatigue problem, cyclic variable-amplitude loads and soil degradation model used in Plaxis are ignored in the paper. However, when cyclic loading is applied on the conductor, the plastic deformation is increasing with water pumping and soil scour around the conductor occurring.

Consequently, there are some tasks should be included for further work:

1) Water pumping influence on the gap between soil and conductor.
2) Plastic deformation occurring when the numble of cyclic loading increasing.
3) Effect of cyclic variable-amplitude.
4) Fatigue problem for conductor.
5) The difference of soil degradation between 2D and 3D.

10 REFERENCE

Lars Olav Grande. “Samvirke Mellom Pel og Jord”, Ph.d. thesis, 1976.

L. Grande, S. Nordal. “PILE-SOIL INTERACTION ANALYSIS ON EFFECTIVE STRESS BASIS”, Recent developments in the design and construction of piles. ICE, London, 1979.

Steinar Nordal. “PHD course Geodynamics lecture notes 2011”, NTNU, 2011.

Amir Kaynia. “PHD course Geodynamics Earthquake_Codes&Practice 2011”, NTNU, 2011.

J.H.Long, Geert Vanneste. “Effects of cyclic lateral loads on piles in sand”, Journal of Geotechnical Engineering, Vol. 120, No.1, 1994.

San-Shyan Lin, Jen-Cheng Liao. “Permanent strains of piles in sand due to cyclic lateral loads”, Journal of Geotechnical and Geoenvironmental Engineering, 1999.

Knut H. Andersen. “Bearing capacity under cyclic loading-offshore, along the coast and on land”, The 21st Bjerrum Lecture, presented in Oslo 23 November 2007.

Knut H. Andersen, Rune Dyvik and Yoshiaki Kikuchi. “Clay Behaviour Under Irregular Cyclic loading”.

Hudson Matlock. “Correlations for design of laterally loaded piles in soft clay”, Offshore Technology Conference, 10.4043/1204-MS , 1970.

Steven L. Kramer. “Geotechnical Earthquake Engineering”, Prentice Hall, 1 edition (28 Dec 1995)

J. Bosboom, M.J.F. Stive. “Coastal Dynamics 1 and 2”, Draft version lecture notes CT4305 TU Delft, 2010.

Matlock H, Reese LC. “Generalized Solutions for Laterally Loaded Piles”, ASCE Soil Mechanics and Foundations Division journal, Volume 86-issue 5, 1960.

Wei Dong Guo, F.H.Lee. “ Load transfer approach for laterally loaded piles”, International journal for numerical and analytical methods in geomechanics, 25:1101-1129, 2001.

Joseph E. Bowles. “FOUNDATION ANALYSIS AND DESIGN”, 2ed Edition, McGraw-Hill, 0-07-006750-3, 1977.

Anil K. Chopra. “Dynamics of structures---Theory and Applications to Earthquake Engineering”, 3rd Edition, Pearson Education, 978-7-302-20218-9, 2007.

Raymond W. Clough, J.Penzien. “Dynamics of Structures”, 2ed Edition, 0070113947, 1993.

V.D.Krolis, J.V.D.Tempel, W.D.Vries. “Evaluation of foundation design for monopile support structures for offshore wind turbines”, DUWIND Offshore Engineering and TU Delft, 2008.

L.C. Reese, W.F. van Impe. “Single pile and pile groups under lateral laoding”, A.A. Balkema, Rotterdam, 2001.

Li Guangxin. “Advanced soil mechanics”, Tsinghua University, 2004.

S.Prakash, H.D.Sharma. “Pile foundation in engineering practice”, WILEY-INTERSCIENCE, 1989.

APPENDIX

Appendix A

Matlab codes for lateral displacement calculation:
(The codes depend on theory of elastic pile in Lars Grande Ph.d. thesis 1976)
There are 3 cases in calculation and 10, 100, 1000 and 10000 cyclic loading are included.

- Case1: 2000Kn horizontal force, 450 tons BOP, with influence of gap.
- Case2: 2000Kn horizontal force, 450 tons BOP, without influence of gap.
- Case3: 2000Kn horizontal force, 250 tons BOP, with influence of gap.

```
% Zhou Zefeng Master Thesis(lateral deflection loop calculation).
% The calculation is named "calloop" for static condition.
% The function will be used for 10, 100, 1000 and 10000 cyclic calculation.

function calloop
% k= constant of soil modulus variation with depth;
% kn= modified soil modulus with depth after each loop calculation;
% h= coefficient in the difference-equation solution;
% g= coefficient in the difference-equation solution;
% E= EI, flexural stiffness of pile, the product of modulus of elasticity
% y= lateral deflection, in meter;
% py(i).u= P-y data from cyclic modified static p-y data, and i is No.
of soil layer.;

% 1) Initially input
py(1).u=[0 0 0 0 0 0 0 0 0 0;0 0 0 0 0 0 0 0 0 0];
py(2).u=[0 0.0298 0.0596 0.0894 0.1192 0.1490 0.1789 0.2086 0.2384
0.2683;0 3408.340 5882.536 7292.537 7987.757 8305.645 8446.895 8508.250
8534.302 8545.461]; % Depth: 50m
py(3).u=[0 0.0323 0.0647 0.0971 0.1295 0.1618 0.1942 0.2266 0.2590 0.291;0
3099.908 5349.465 6631.993 7263.922 7553.285 7681.164 7737.170 7761.439
7771.706];  % Depth: 40.45m
py(4).u=[0 0.0323 0.0647 0.0971 0.1295 0.1618 0.1942 0.2266 0.2590
0.2914;0 2681.733 4628.860 5737.771 6284.758 6534.917 6645.994 6693.599
6715.068 6723.469];  % Depth: 35m
py(5).u=[0 0.0323 0.0647 0.0971 0.1295 0.1618 0.1942 0.2266 0.2590
0.2914;0 2333.56 4027.73 4992.89 5468.94 5686.43 5782.57 5824.57 5842.31
5850.71];  % Depth: 30.45m
py(6).u=[0 0.032 0.064 0.097 0.129 0.161 0.194 0.226 0.259 0.291;0 1915.39
3306.19 4098.67 4488.84 4668.06 4746.47 4781.00 4795.94 4802.47];  % Depth:
25m
py(7).u=[0 0.032 0.064 0.097 0.129 0.161 0.194 0.226 0.259 0.291;0
```

```
1567.22 2705.06 3353.80 3673.03 3819.58 3883.98 3911.98 3924.12
3929.72];  % Depth: 20.45m
py(8).u=[0 0.032 0.064 0.097 0.129 0.161 0.194 0.226 0.259 0.291;0 1149.047
1983.530 2459.578 2693.868 2800.278 2847.883 2868.418 2877.753
2881.486];  % Depth: 15m
py(9).u=[0 0.0286 0.0573 0.0860 0.1147 0.1434 0.1722 0.2009 0.2295
0.2582;0 709.9639 1225.588 1518.684 1663.365 1729.638 1759.508 1771.642
1777.243 1780.043];  % Depth: 10.45m
py(10).u=[0 0.0154 0.0308 0.0462 0.0616 0.0770 0.0924 0.1078 0.1233
0.1387;0 182.298 314.657 390.078 427.229 444.310 451.778 455.045 456.445
457.098];  %  Depth: 5m
py(11).u=[0 0.0110 0.0220 0.0329 0.0439 0.0549 0.0659 0.0769 0.0878
0.0988;0 82.664 142.72 176.88 193.68 201.43 204.88 206.38 206.94
207.22];  % Depth: 3.18m
py(12).u=[0 0.00876 0.01753 0.02629 0.03505 0.04382 0.05258 0.06135
0.07011 0.07887;0 47.1380 81.3574 100.810 110.424 114.904 116.771 117.611
117.985 118.171]; % Depth: 2.27m
py(13).u=[0 0.00654 0.01309 0.01964 0.02620 0.03274 0.03929 0.04584
0.0524 0.0589;0 21.132 36.478 45.224 49.527 51.497 52.374 52.757 52.915
52.990]; % Depth: 1.36m
dt=[1.11 0.45 9.55 5.45 4.55 5.45 4.55 5.45 4.55 5.45 1.82 0.91 0.91 1.36
1 1]; % 16 elements
ki=[0 1340.257672 214.2282557 600.4319757 885.7022409 790.180751
346.9688515 396.1541299 1047.606201 485.0738116 222 126.6 56.77 0]; % 14
elements

% k matrix
k=zeros(5000,14);
for i=1:14
   k(1,i)=ki(i);
end
v=zeros(5000,14);
g=zeros(5000,14);
h=zeros(5000,26);
kn=zeros(5000,14);
E=7194041.4;  %E is the E*I
Fh=2000;
Mb=18000;

 % 2) g matrix calculation
for i=1:13
    g(1,i)=(k(1,i)*dt(i)^4)/E;
end
g(1,14)=0;
```

```
 % 3) h matrix calculation
h(1,1)=2/(2+g(1,2));
h(1,2)=2*h(1,1);
h(1,3)=1/(5+g(1,3)-4*h(1,1));
h(1,4)=(4-h(1,2))*h(1,3);
h(1,5)=1/(6+g(1,4)-h(1,1)+h(1,4)*(h(1,2)-4));
h(1,6)=(4-h(1,3)*(4-h(1,2)))*h(1,5);
for i=1:10
    j=2*i;
    h(1,5+j)=1/(6+g(1,4+i)-h(1,1+j)+h(1,4+j)*(h(1,2+j)-4));
    h(1,6+j)=(4-h(1,3+j)*(4-h(1,2+j)))*h(1,5+j);
end


% 4) pile top lateral deformation (v) calculation (top(element 13) to
tip(element 1))
jt=(Mb*dt(14)^2)/E;fprintf('jt=%d\n',jt)
jf=(2*Fh*dt(14)^3)/E;fprintf('jf=%d\n',jf)
a2=jt/(1-h(1,23));fprintf('a2=%d\n',a2)
b2=(2-h(1,24))/(1-h(1,23));fprintf('b2=%d\n',b2)
a1=(a2*h(1,26))/h(1,25);fprintf('a1=%d\n',a1)
b1=(b2*h(1,26)-1)/h(1,25);fprintf('b1=%d\n',b1)
a3=a2*h(1,23);fprintf('a3=%d\n',a3)
b3=h(1,24)-b2*h(1,23);fprintf('b3=%d\n',b3)
a4=a3*h(1,22);fprintf('a4=%d\n',a4)
b4=b3*h(1,22)-h(1,21);fprintf('b4=%d\n',b4)
v(1,13)=(jf+(a1-2*a2-a3+a4))/(b4-2*b3+2*b2-b1);
v(1,12)=b3*v(1,13)-a3;
v(1,11)=b4*v(1,13)-a4;
for i=-sort(-(1:10))
    v(1,i)=h(1,i*2)*v(1,i+1)-h(1,2*i-1)*v(1,i+2);
end
v(1,2)=h(1,4)*v(1,3)-h(1,3)*v(1,4);
v(1,1)=h(1,2)*v(1,2)-h(1,1)*v(1,3);
v=abs(v);

% 5) k modified from table which is Interpolation function
for i=2:13
    if v(1,i-1)<=py(i).u(1,2)

kn(1,i)=((py(i).u(2,2)-py(i).u(2,1))*(v(1,i-1)-py(i).u(1,1)))/(py(i).
u(1,2)-py(i).u(1,1))+py(i).u(2,1);
    else if  py(i).u(1,3)>= v(1,i-1)>py(i).u(1,2)
```

```
kn(1,i)=((py(i).u(2,3)-py(i).u(2,2))*(v(1,i-1)-py(i).u(1,2)))/(py(i).
u(1,3)-py(i).u(1,2))+py(i).u(2,2);
       else if py(i).u(1,4)>= v(1,i-1)>py(i).u(1,3)

kn(1,i)=((py(i).u(2,4)-py(i).u(2,3))*(v(1,i-1)-py(i).u(1,3)))/(py(i).
u(1,4)-py(i).u(1,3))+py(i).u(2,3);
          else if py(i).u(1,5)>= v(1,i-1)>py(i).u(1,4)

kn(1,i)=((py(i).u(2,5)-py(i).u(2,4))*(v(1,i-1)-py(i).u(1,4)))/(py(i).
u(1,5)-py(i).u(1,4))+py(i).u(2,4);
             else if py(i).u(1,6)>= v(1,i-1)>py(i).u(1,5)

kn(1,i)=((py(i).u(2,6)-py(i).u(2,5))*(v(1,i-1)-py(i).u(1,5)))/(py(i).
u(1,6)-py(i).u(1,5))+py(i).u(2,5);
                 else if py(i).u(1,7)>= v(1,i-1)>py(i).u(1,6)

kn(1,i)=((py(i).u(2,7)-py(i).u(2,6))*(v(1,i-1)-py(i).u(1,6)))/(py(i).
u(1,7)-py(i).u(1,6))+py(i).u(2,6);
                    else if  py(i).u(1,8)>= v(1,i-1)>py(i).u(1,7)

kn(1,i)=((py(i).u(2,8)-py(i).u(2,7))*(v(1,i-1)-py(i).u(1,7)))/(py(i).
u(1,8)-py(i).u(1,7))+py(i).u(2,7);
                       else if  py(i).u(1,9)>= v(1,i-1)>py(i).u(1,8)

kn(1,i)=((py(i).u(2,9)-py(i).u(2,8))*(v(1,i-1)-py(i).u(1,8)))/(py(i).
u(1,9)-py(i).u(1,8))+py(i).u(2,8);
                          else if  py(i).u(1,10)>=
v(1,i-1)>py(i).u(1,9)

kn(1,i)=((py(i).u(2,10)-py(i).u(2,9))*(v(1,i-1)-py(i).u(1,9)))/(py(i)
.u(1,10)-py(i).u(1,9))+py(i).u(2,9);
                             else
                                kn(1,i)=py(i).u(2,10);
                             end

                          end

                       end

                    end

                 end
```

```
            end

        end

    end

end
end
kn(1,1)=0;
kn(1,14)=0;

% 6) loop calculation
  for zz=2:3140

    for i=1:14
        k(zz,i)=kn(zz-1,i);
    end
    % g matrix calculation
    for i=1:13
        g(zz,i)=(k(zz,i)*dt(i)^4)/E;
    end
    g(zz,14)=0;

    % h matrix calculation
    h(zz,1)=2/(2+g(zz,2));
    h(zz,2)=2*h(zz,1);
    h(zz,3)=1/(5+g(zz,3)-4*h(zz,1));
    h(zz,4)=(4-h(zz,2))*h(zz,3);
    h(zz,5)=1/(6+g(zz,4)-h(zz,1)+h(zz,4)*(h(zz,2)-4));
    h(zz,6)=(4-h(zz,3)*(4-h(zz,2)))*h(zz,5);
    for i=1:10
        j=2*i;
        h(zz,5+j)=1/(6+g(zz,4+i)-h(zz,1+j)+h(zz,4+j)*(h(zz,2+j)-4));
        h(zz,6+j)=(4-h(zz,3+j)*(4-h(zz,2+j)))*h(zz,5+j);
    end

    % v calculation (top(13) to tip(1))
    jt=(Mb*dt(14)^2)/E;
    jf=(2*Fh*dt(14)^3)/E;
    a2=jt/(1-h(zz,23));
    b2=(2-h(zz,24))/(1-h(zz,23));
    a1=(a2*h(zz,26))/h(zz,25);
    b1=(b2*h(zz,26)-1)/h(zz,25);
```

```
    a3=a2*h(zz,23);
    b3=h(zz,24)-b2*h(zz,23);
    a4=a3*h(zz,22);
    b4=b3*h(zz,22)-h(zz,21);
    v(zz,13)=(jf+(a1-2*a2-a3+a4))/(b4-2*b3+2*b2-b1);
    v(zz,12)=b3*v(zz,13)-a3;
    v(zz,11)=b4*v(zz,13)-a4;
    for i=-sort(-(1:10))
        v(zz,i)=h(zz,i*2)*v(zz,i+1)-h(zz,2*i-1)*v(zz,i+2);
    end
    v(zz,2)=h(zz,4)*v(zz,3)-h(zz,3)*v(zz,4);
    v(zz,1)=h(zz,2)*v(zz,2)-h(zz,1)*v(zz,3);

    v=abs(v);

    %
    kn(zz,14)=0;
    kn(zz,1)=0;
    for i=2:13
    if v(zz,i-1)<=py(i).u(1,2)

kn(zz,i)=((py(i).u(2,2)-py(i).u(2,1))*(v(zz,i-1)-py(i).u(1,1)))/(py(i
).u(1,2)-py(i).u(1,1))+py(i).u(2,1);
    else if  py(i).u(1,3)>= v(zz,i-1)>py(i).u(1,2)

kn(zz,i)=((py(i).u(2,3)-py(i).u(2,2))*(v(zz,i-1)-py(i).u(1,2)))/(py(i
).u(1,3)-py(i).u(1,2))+py(i).u(2,2);
       else if py(i).u(1,4)>= v(zz,i-1)>py(i).u(1,3)

kn(zz,i)=((py(i).u(2,4)-py(i).u(2,3))*(v(zz,i-1)-py(i).u(1,3)))/(py(i
).u(1,4)-py(i).u(1,3))+py(i).u(2,3);
          else if py(i).u(1,5)>= v(zz,i-1)>py(i).u(1,4)

kn(zz,i)=((py(i).u(2,5)-py(i).u(2,4))*(v(zz,i-1)-py(i).u(1,4)))/(py(i
).u(1,5)-py(i).u(1,4))+py(i).u(2,4);
             else if py(i).u(1,6)>= v(zz,i-1)>py(i).u(1,5)

kn(zz,i)=((py(i).u(2,6)-py(i).u(2,5))*(v(zz,i-1)-py(i).u(1,5)))/(py(i
).u(1,6)-py(i).u(1,5))+py(i).u(2,5);
                else if py(i).u(1,7)>= v(zz,i-1)>py(i).u(1,6)

kn(zz,i)=((py(i).u(2,7)-py(i).u(2,6))*(v(zz,i-1)-py(i).u(1,6)))/(py(i
).u(1,7)-py(i).u(1,6))+py(i).u(2,6);
                    else if  py(i).u(1,8)>= v(zz,i-1)>py(i).u(1,7)
```

```
kn(zz,i)=((py(i).u(2,8)-py(i).u(2,7))*(v(zz,i-1)-py(i).u(1,7)))/(py(i
).u(1,8)-py(i).u(1,7))+py(i).u(2,7);
                        else if  py(i).u(1,9)>= v(zz,i-1)>py(i).u(1,8)

kn(zz,i)=((py(i).u(2,9)-py(i).u(2,8))*(v(zz,i-1)-py(i).u(1,8)))/(py(i
).u(1,9)-py(i).u(1,8))+py(i).u(2,8);
                            else if  py(i).u(1,10)>=
v(zz,i-1)>py(i).u(1,9)

kn(zz,i)=((py(i).u(2,10)-py(i).u(2,9))*(v(zz,i-1)-py(i).u(1,9)))/(py(
i).u(1,10)-py(i).u(1,9))+py(i).u(2,9);
                                else
                                    kn(zz,i)=py(i).u(2,10);
                                end
                            end
                        end
                    end
                end
            end
        end
    end
    end

 end
q=3140;
fprintf('final kn matrix is %d    %d\n',kn(q,2),kn(q-1,2))
fprintf('final kn matrix is %d    %d\n',kn(q-2,2),kn(q-3,2))
fprintf('final kn matrix is %d    %d\n',kn(q-4,2),kn(q-5,2))

fprintf('final lateral deflection is %d m\n',v(3140,13))
```

Appendix B

The codes depend on dynamic theory and eigen-value theory. Moreover the code is performed in 6 cases:

- Case1:450 tons BOP, without scour.
- Case2:450 tons BOP +water influence (50% total weight of BOP), without scour.
- Case3:450 tons BOP, with scour.
- Case4: 450 tons BOP +water influence (50% total weight of BOP), with scour.
- Case5: 250 tons with scour.
- Case6: 250 tons BOP +water influence (50% total weight of BOP), with scour.

```
% Zhou Zefeng Master Thesis(Natural frequency analysis calculation).
% The calculation is named "eigenvalue" for static condition.
% The function will be used for 10, 100, 1000 and 10000 cyclic calculation
with two BOP conditions
% This calculation is BOP=450t without scour condition
function eignvalue
E=7194041.4;% E is E*I
L=[3 1.36 0.91 0.91 1.82 5.45 4.55 5.45 4.55 5.45 4.55 5.45 9.55]; % length
of element of conductor
kn=[0 52.99 118.171 207.22 451.9439 970.489 419.8326 237.4274 646.8155
747.8778 532.3669 113.3101 463.3];  % soil modulus for different depth
mo=1.654735635;% average mass per meter(conductor)
k=zeros(28,28);
m=zeros(28,28);

% 1) Initial Total Mass Matrix
m(1,1)=451.8438483;
m(1,2)=-2699.21991;
m(2,2)=22950.4255 ;
m(2,1)=m(1,2);
m(1,3)=0.638255173;
m(1,4)=-0.46096207;
m(2,3)=0.46096207;
m(2,4)=-0.319127587;
m(3,1)=m(1,3);
m(4,1)=m(1,4);
m(3,2)=m(2,3);
```

```
m(4,2)=m(2,4);

% odd element
for i=1:12
    n=2*i+1;
    m(n,n-2)=mo*L(i)*54/420;
    m(n,n-1)=(mo*L(i)*13*L(i))/420;
    m(n,n)=(mo*L(i)*156/420)+(mo*L(i+1)*156/420);
    m(n,n+1)=(mo*L(i)*-22*L(i)/420)+(mo*L(i+1)*22*L(i+1)/420);
    m(n,n+2)=mo*L(i+1)*54/420;
    m(n,n+3)=(mo*L(i+1)*-13*L(i+1))/420;
end

% even element
for i=2:13
    n=i*2;
    m(n,n-3)=(mo*L(i-1)*-13*L(i-1))/420;
    m(n,n-2)=(mo*L(i-1)*-13*L(i-1))/420;
    m(n,n-1)=(mo*L(i-1)*-22*L(i-1)/420)+(mo*L(i)*22*L(i)/420);
    m(n,n)=(mo*L(i-1)*4*L(i-1)*L(i-1)/420)+(mo*L(i)*4*L(i)*L(i)/420);
    m(n,n+1)=(mo*L(i)*13*L(i))/420;
    m(n,n+2)=(mo*L(i)*-3*L(i)*L(i))/420;
end
m(28,27)=-7.905125209;
m(27,27)=5.869583687;
m(27,28)=-7.905125209;
m(27,26)=4.671210351;
m(26,27)=4.671210351;
m(27,25)=2.031778968;
m(25,27)=2.031778968;
m(28,28)=13.72617195;
m(28,26)=-10.29462896;
m(26,28)=-10.29462896;
m(28,25)=-4.671210351;
m(25,28)=-4.671210351;
fprintf('the m matrix %d\n',m)

% 2) Initial Total Stiffness Matrix
for i=1:12
    n=2*i+1;
    k(n,n-2)=(-6*2*E)/((L(i))^3);
    k(n,n-1)=(-3*2*E)/((L(i))^2);
    k(n,n)=(2*E*6)/((L(i))^3)+(2*E*6)/((L(i+1))^3)+kn(i);
    k(n,n+1)=(2*E*-3*L(i))/((L(i))^3)+(2*E*3*L(i+1))/((L(i+1))^3);
```

```
    k(n,n+2)=(-6*2*E)/((L(i+1))^3);
    k(n,n+3)=(2*E*3*L(i+1))/((L(i+1))^3);
end

for i=2:13
    n=i*2;
    k(n,n-3)=(3*L(i-1)*2*E)/((L(i-1))^3);
    k(n,n-2)=(L(i-1)*L(i-1)*2*E)/((L(i-1))^3);
    k(n,n-1)=(-3*L(i-1)*E*2)/((L(i-1))^3)+(3*L(i)*E*2)/((L(i))^3);

k(n,n)=(2*L(i-1)*L(i-1)*2*E)/((L(i-1))^3)+(2*L(i)*L(i)*2*E)/((L(i))^3
);
    k(n,n+1)=(-3*L(i)*E*2)/((L(i))^3);
    k(n,n+2)=(2*L(i)*L(i)*2*E)/((L(i))^3);
end
k(1,1)=(6*2*E)/((L(1))^3);
k(1,2)=(3*L(1)*2*E)/((L(1))^3);
k(2,1)=k(1,2);
k(2,2)=(4*L(1)*L(1)*E)/((L(1))^3);
k(1,3)=k(3,1);
k(1,4)=k(4,1);
k(2,3)=k(3,2);
k(2,4)=k(4,2);

k(28,27)=(-6*L(13)*E)/((L(13))^3);
k(27,27)=(12*E)/((L(13))^3)+kn(13);
k(27,28)=k(28,27);
k(27,26)=k(26,27);
k(27,25)=k(25,27);
k(28,28)=(4*L(13)*L(13)*E)/((L(13))^3);
k(28,26)=k(26,28);
k(28,25)=k(25,28);
fprintf('the k matrix %d\n',k)

% 3) The eigen value calculation (Eigenfrequencies calculation)
[Eigenvec,Eigenfrec] = eig(k,m);
Eigenfrec=sqrt(Eigenfrec)/(2*3.14);

fprintf('the Eigenfrec matrix %d\n',Eigenfrec)
```

Appendix C

Consistent element matrices for plane frame element:

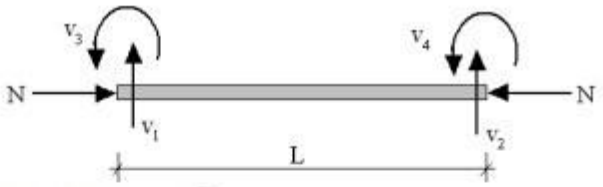

$$\mathbf{k} = \frac{EI}{L^3}\begin{bmatrix} 12 & -12 & 6L & 6L \\ -12 & 12 & -6L & -6L \\ 6L & -6L & 4L^2 & 2L^2 \\ 6L & -6L & 2L^2 & 4L^2 \end{bmatrix}$$

$$\mathbf{m} = \frac{ml}{420}\begin{bmatrix} 156 & 54 & 22L & -13L \\ 54 & 156 & 13L & -22L \\ 22L & 13L & 4L^2 & -3L^2 \\ -13L & -22L & -3L^2 & 4L^2 \end{bmatrix}$$

$$\mathbf{k}_G = \frac{N}{30L}\begin{bmatrix} 36 & -36 & 3L & 3L \\ -36 & 36 & -3L & -3L \\ 3L & -3L & 4L^2 & -L^2 \\ 3L & -3L & -L^2 & 4L^2 \end{bmatrix}$$

Appendix D

In the paper, the soil resistance is considered as springs, and the depth have been chosen below:

Table D-1 the soil spring depth

Depth (m)
0
1.36
2.27
3.18
5
10.45
15
20.45
25
30.45
35
40.45
50

After loop calculation (chapter 6), we can get the stiffness of spring in different depth:

- Case1: 2000Kn horizontal force, 450 tons BOP, with influence of gap.
- Case2: 2000Kn horizontal force, 450 tons BOP, without influence of gap.
- Case3: 2000Kn horizontal force, 250 tons BOP, with influence of gap.

CASE 1:

1) Static condition

Stiffness(kN/m2)	Depth(m)
0	0
0	1.36
118.171	2.27
207.22	3.18
451.9343	5
967.4704	10.45
409.7954	15
255.4521	20.45
672.1029	25
778.9073	30.45
564.1919	35
141.3768	40.45
440.2453	50

2) **10 cyclic loading condition**

Stiffness(kN/m2)	Depth(m)
0	0
0	1.36
118.171	2.27
207.22	3.18
451.9883	5
953.9619	10.45
346.8604	15
390.0841	20.45
896.0729	25
1120.804	30.45
1039.228	35
785.3697	40.45
440.2984	50

3) 100 cyclic loading condition

Stiffness(kN/m2)	Depth(m)
0	0
0	1.36
108.99	2.27
193.425	3.18
420.3499	5
877.9851	10.45
345.7706	15
300.0138	20.45
755.4552	25
970.0844	30.45
897.763	35
662.0893	40.45
314.9215	50

4) 10000 cyclic loading condition

Stiffness(kN/m2)	Depth(m)
0	0
0	1.36
96.1067	2.27
168.528	3.18
363.3419	5
742.6128	10.45
350.898	15
142.7404	20.45
504.3357	25
670.1551	30.45
599.8448	35
382.6744	40.45
279.12761	50

Case 2:

1) Static condition

Stiffness(kN/m2)	Depth(m)
0	0
52.99	1.36
118.171	2.27
207.22	3.18
451.9439	5
970.489	10.45
419.8326	15
237.4274	20.45
646.8155	25
747.8778	30.45
532.3669	35
113.3101	40.45
463.3	50

2) **10 cyclic loading condition**

Stiffness(kN/m2)	Depth(m)
0	0
52.99	1.36
118.171	2.27
207.22	3.18
451.9827	5
953.7502	10.45
346.7795	15
389.9312	20.45
895.7299	25
1120.303	30.45
1038.599	35
784.5856	40.45
439.2965	50

3) 100 cyclic loading condition

Stiffness(kN/m2)	Depth(m)
0	0
49.462	1.36
108.99	2.27
193.425	3.18
420.339	5
877.8066	10.45
345.7348	15
299.8054	20.45
755.0178	25
969.4084	30.45
896.8542	35
660.8836	40.45
313.4252	50

4) 10000 cyclic loading condition

Stiffness(kN/m2)	Depth(m)
0	0
43.0961	1.36
96.1067	2.27
168.528	3.18
363.3343	5
742.4741	10.45
350.8104	15
142.7229	20.45
504.2493	25
670.0476	30.45
599.7671	35
382.6588	40.45
279.19207	50

Case 3:

1) Static condition

Stiffness(kN/m2)	Depth(m)
0	0
0	1.36
118.171	2.27
207.22	3.18
437.964	5
791.7293	10.45
306.1203	15
253.6279	20.45
652.203	25
831.4355	30.45
763.3047	35
546.4214	40.45
250.8753	50

2) **10 cyclic loading condition**

Stiffness(kN/m2)	Depth(m)
0	0
0	1.36
118.171	2.27
207.22	3.18
437.964	5
791.7293	10.45
306.1203	15
253.6279	20.45
652.203	25
831.4355	30.45
763.3047	35
546.4214	40.45
250.8753	50

3) 100 cyclic loading condition

Stiffness(kN/m2)	Depth(m)
0	0
0	1.36
108.99	2.27
193.425	3.18
405.8463	5
728.5054	10.45
309.4768	15
173.5124	20.45
523.7081	25
684.6468	30.45
615.9201	35
405.9884	40.45
109.9646	50